Materials Advances

ROYAL SOCIETY OF CHEMISTRY

REVIEW

View Article Online
View Journal

Cite this: DOI: 10.1039/d6ma00272b

Carbon dot-integrated hydrogel systems for solar-driven water evaporation and purification: materials design, mechanisms, and recent advances

Srishti Bardhan,[a] Debsankar Sahoo,[a] Manab Kalita,[b] Priya Deb,[a] Tamal Basu,[a] Sanchayita Rajkhowa,[c] Chirantan Kar*[a] and Pradip K. Sukul*[a]

Water plays a pivotal role as a resource for ecological sustenance. Escalating concerns about water scarcity have intensified research and scientific focus on next-generation water-treatment methods. Solar-driven water purification offers a sustainable pathway to reclaim freshwater resources and alleviate shortages. This review paper critically examines carbon dot (CD)-integrated hydrogel systems for solar water evaporation, emphasizing materials design, photothermal mechanisms and recent performance advances. First, the mechanism of solar water evaporation is discussed, followed by the photothermal properties of carbon dots, thereby highlighting recent developments in carbon dot-based solar water evaporators. Next, the various characteristics of hydrogels including their photothermal properties are elaborated. While reviewing the advantages of hydrogel-based solar water evaporators as well as the synergistic effects of carbon dot (CD)-based hydrogel composites, the recent advancements in CD–hydrogel composites are also overviewed. The key points on challenges in achieving long-term durability, multi-functional pollutant removal and prevention of salt crystallization are summarized, along with recommended future research directions. Efficient energy confinement facilitated by solar vapor generation can progress with updated designs, which can turn out to be evolutionary towards sustainability.

Received 26th February 2026,
Accepted 1st June 2026

DOI: 10.1039/d6ma00272b

rsc.li/materials-advances

[a] Department of Chemistry, Amity Institute of Applied Sciences, Amity University Kolkata, Action Area-II, Kadampukur, New Town, Rajarhat, Kolkata-700135, India. E-mail: sukul.ochem@gmail.com, pksukul@kol.amity.edu
[b] Department of Chemistry, Indian Institute of Technology Guwahati, Guwahati, Assam-781039, India
[c] Department of Chemistry, Haflong Government College, Dima Hasao, Assam-788819, India

1. Introduction

Water is essential for life. Despite the abundant presence of water, only 0.02% of the total water is accessible to people, plants and animals. The surge in population growth, economic development, industrialisation, agricultural advancement and

Srishti Bardhan

Srishti Bardhan received her bachelor's and master's degree in Chemistry from Nagaland University and The Assam Royal Global University respectively. She is presently enrolled in a PhD program in Chemistry at Amity University Kolkata. Her research focuses on the development of advanced polymer nanocomposites as innovative solutions for sustainable water resources.

Debsankar Sahoo

Debsankar Sahoo completed his master's degree in Chemistry from Amity University Kolkata and is currently pursuing his PhD at the same institution. His research interests center on the development and characterization of polymer nanocomposites and their advanced applications.

the climate crisis led to an eightfold increase in the demand for freshwater between 1990 and 2010.[1] In spite of the rapidly evolving economic aspects, it is predicted that by 2050, global water demand will elevate by 20–30%, approximately 5500 to 6000 km^3 per year, which is an alarming call for all. This critical future state of affairs is expected to further worsen the public health crisis. The present annual withdrawals globally are lower than the annual discharge. This global concern is expected to face a surge in the near future, mostly depending on both climatic and socio-economic changes.[2] In alignment with the perception of the United Nations Sustainable Development Goals, ensuring sustainable water security in the forthcoming years necessitates the advancement of innovative water treatment technologies that can employ inexhaustible water resources while being resilient and adaptable under all circumstances.[3] A new terminology introduced as 'clean-water scarcity' presents an overall overview accounting for both good quantity and quality of water based on the global nitrogen pollution rate under different spectra of climatic and socio-economic advancements. Few initiatives have been implemented to preserve freshwater resources: (a) sustainable utilization of water and reduction of unnecessary wastage of water, (b) purifying wastewater and reusing and recycling it to improve the usage rate of water resources and (c) acquiring usable water from other sources, including desalting of seawater and condensation of atmospheric water.[4] Further initiatives and innovations that make potable water available from contaminated or polluted sources must be sustainable and environmentally benign and must not lead to additional strain on clean water accessibility. The trade-off between energy and water, known as the energy-water nexus, cannot be avoided. In this respect, solar vapor generation using solar energy is a propitious sustainable strategy.[5] A number of reports have shown the combination of carbon dots (CDs) and hydrogels to produce newer functional polymers. In order to facilitate the hydrogels to harvest solar energy, they should be modified with such solar absorbers that ace in interfacial heating rather than bottom or bulk heating, thereby enhancing the efficacy {Fig. 1(a)–(c)}. Carbon dots with innocuity and its cost-effective sources carry sufficient hydroxyl and carboxyl groups on the surface that can be used as all-purpose constituents in the design of solar evaporators.[6] Therein, CDs have various applications in numerous fields such as biological imaging,[7] catalysis,[8] optoelectronic devices[9] and detection.[10] Specifically, the CDs play salient roles in the hydrogel, further improvising its mechanical firmness, boosting the purification of water through enhanced adsorption. The hydrogel serves as a solar-mediated vehicle for water purification.[11] For the need of overcoming the heat of vaporization, the rate of water production *via* initiatives inculcating solar power remains significantly deficient to meet the overpouring demands. Surmounting this loophole is crucial for establishing solar purification as a 'one-size-fits-all' solution for accessibility to cleaner water.[12] This review critically surveys the

Manab Kalita

Manab Kalita is currently a Research Fellow in the Department of Chemistry at the Indian Institute of Technology Guwahati, India. His research focuses on the development of hybrid organic–inorganic semiconductors and electronic devices, with particular emphasis on organic field-effect transistors (OFETs) and optoelectronic applications.

Priya Deb

Priya Deb is currently pursuing her PhD at Amity University Kolkata, specializing in polymer chemistry and nanomaterials. Her research focuses on the development and characterization of advanced polymer-based systems with applications in sustainable materials and nanotechnology.

Pradip K. Sukul

Dr Pradip K. Sukul is an Associate Professor in the Department of Chemistry at Amity University Kolkata, India. He received his PhD in Chemistry from the Indian Association for the Cultivation of Science (IACS) and Jadavpur University, Kolkata. He has conducted research at the National Institute for Materials Science (NIMS), Japan, and Chimie ParisTech-PSL University, France, and served as a DST INSPIRE Faculty Fellow at National Institute of Technology, Patna. His research interests include metal–peptide chemistry, supramolecular chemistry, functional nanomaterials, biomaterials, and sustainable materials for energy, environmental, and biomedical applications.

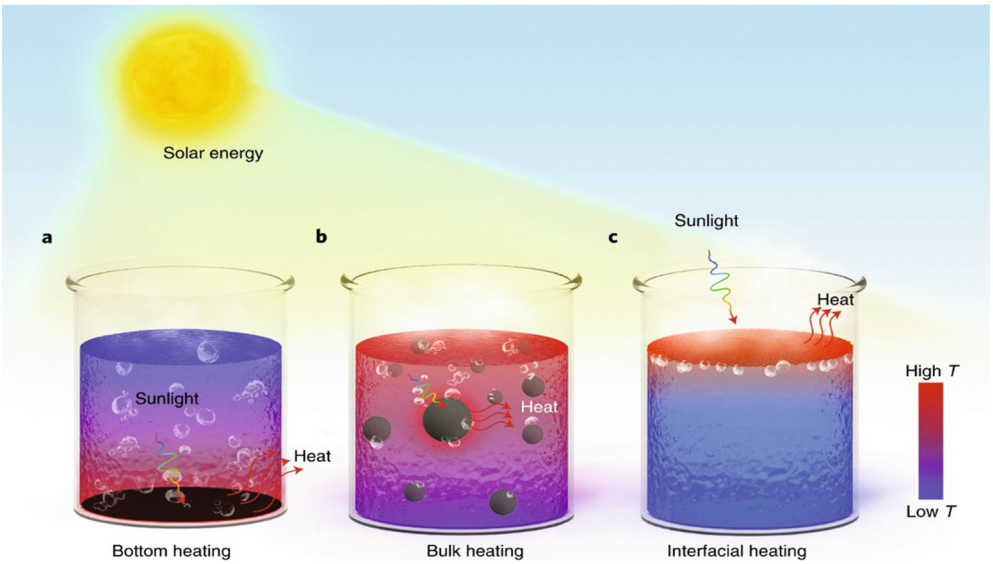

Fig. 1 Solar-driven evaporation *via* three principal thermal pathways: (a) bottom heating, (b) volumetric (bulk) heating and (c) interfacial heating. Reprinted with permission from ref. 13. Copyright 2022 Wiley-VCH GmbH.

advanced and emerging best-in class developments in the fundamental components of solar-induced evaporation systems and elucidates its diverse application domains, thereby providing a comprehensive assessment of material engineering approaches employed to elevate the evaporation efficiency. It examines how the synergistic integration of carbon dots as functional additives with sophisticated structural architectures – covering both material and system level designs – has led to consistent performance optimization. Finally, this review identifies critical scientific challenges and highlights prospective research directions essential for advancing both fundamental understanding and large-scale industrial deployment of solar-driven interfacial evaporation technologies.

2. Mechanism of solar water evaporation

The mechanism of solar steam generation relies on efficient solar absorbers that convert sunlight into localized heat on a tailored evaporation surface. Structural design and surface engineering enhance water transport and vapor escape while strategies like reducing evaporation enthalpy and optimizing heat distribution improve energy utilization. Additionally, proper thermal insulation lowers heat loss to the bulk water, maximizing the overall evaporation efficacy.

2.1. Solar absorbing materials

Solar-mediated interfacial evaporation depends on strategically selected photothermal materials to elevate sunlight-to-heat conversion by localizing absorbers at the evaporation interface, thereby reducing material consumption, minimizing heat loss and enhancing the energy efficiency.[14,15] Photothermal conversion occurs *via* photon absorption, excitation of charge carriers and subsequent relaxation processes that dissipate heat into the surrounding medium for vapor generation,[16] and commonly employed absorbers comprise metal nanoparticles, semiconductors, conjugated polymers and carbon-based systems.[17–19]

2.1.1. Carbon-derived materials. Carbon-derived materials are extensively utilized across energy and environmental domains[20] owing to their low cost, structural diversity and exceptional stability. Their intrinsic broad-spectrum solar absorption, akin to blackbody radiation, renders them highly effective for solar evaporation applications.[21] Upon solar irradiation, these materials convert absorbed light into heat *via* lattice vibrations, enabling efficient photothermal conversion.[22] They are classified into biomass-derived carbons (biochar)[23–25] – carbon dots (CDs), carbon nanosheets,[26] carbon nanotubes[27] and porous carbon[28] (Table 1). Carbon-based materials inherently black in nature exhibit prominent broadband solar absorption through light-to-thermal conversion processes involving electron excitation followed by quick thermalization *via* electron–electron and electron–phonon scattering. Among the various carbonaceous materials, graphite, hollow carbon spheres and reduced graphene oxide demonstrate solar absorptivity and processability. The solar-to-vapor conversion mechanism in graphene is elucidated in Fig. 2a, arising from its unique electronic band structure and ultrafast carrier dynamics. When broadband solar radiation is incident on monolayer graphene, photons are absorbed across a broad spectral range due to its zero bandgap and linear energy-momentum dispersion. As shown, the valence band (green cone) and conduction band (grey cone) meet at a point, allowing the excitation of electrons virtually without energy threshold. Consequently, incident photons promote electrons from the valence band to higher energy states in the conduction band while leaving behind holes in the valence band. After

Table 1 Comparative analysis of different carbon-based materials[23–28]

Characteristics	Carbon nanotubes (CNTs)	Carbon nanosheets (CNSs)	Porous carbon (PC)	Carbon dots (CDs)	Advantages of CDs over other materials
Dimensions	1D (tubular)	2D (planar)	3D (porous network)	0D (quasi-spherical)	0D structure offers high surface-to-volume ratio and biocompatibility
Luminescence	In general, negligible	Generally negligible	Negligible	Strong and adjustable photoluminescence	Tunable optical properties enhance surface engineering
Dispersibility	Poor (tends to aggregate)	Poor (tends to restack)	Variable (insoluble)	High (water-soluble)	Abundant surface functional groups offer excellent water solubility
Core applications	Conductivity	Supercapacitors and catalysis	Adsorption and energy	Wastewater treatment, bioimaging and sensing	Efficient catalysts in environmental remediation, less toxic and sustainable material
Cost of synthesis	High (chemical vapor deposition required)	Moderate to high	Low to moderate	Very low (bio-based)	Sustainable material in replacement of expensive alternatives using cost-effective and green methods

excitation, the system enters a non-equilibrium state with high-energy charge carriers. The electrons go through electron–electron scattering, followed by energy redistribution. Subsequently, energy is dissipated through electron–phonon coupling, where the excited electrons transfer energy to the phonons of graphene. This process accounts for the conversion of absorbed photon energy into thermal energy. The heat generated gets localized on the graphene surface and can be transferred to water assisting solar evaporation.[29]

In Fig. 2b, a double-layered system comprising a floating carbon foam and an exfoliated graphite layer achieving 97% solar absorbing capacity across 250–2250 nm is presented, while their cost factor remains a limiting factor for their large-scale application. The solar irradiance spectrum is

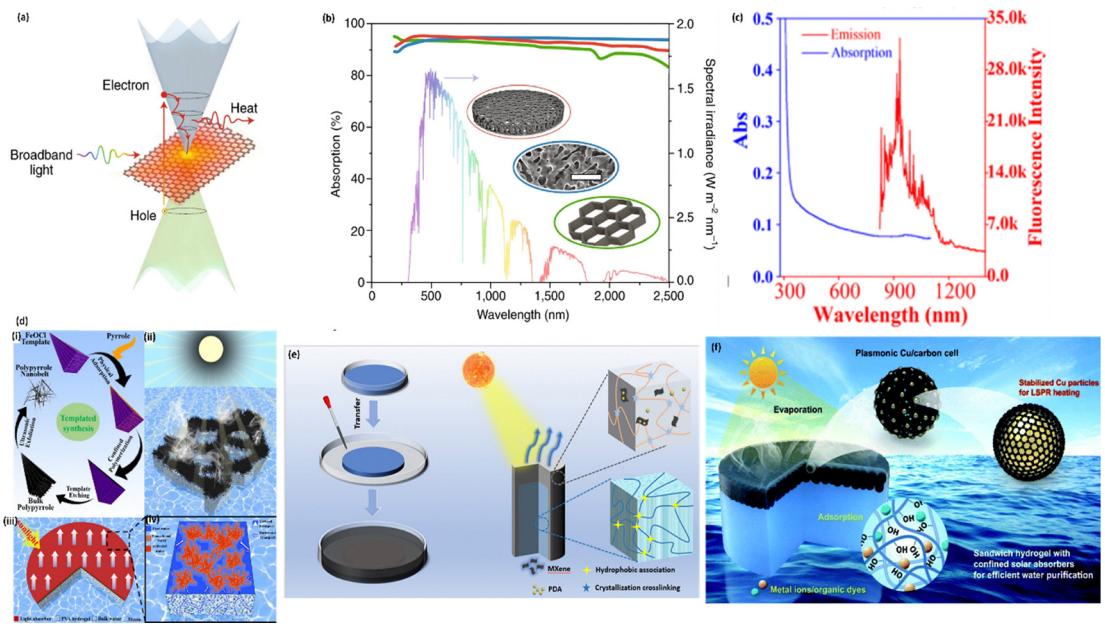

Fig. 2 (a) Solar-thermal conversion mechanism in monolayer graphene: incident sunlight excites electrons from the valence band (green cone) to the conduction band (grey cone) and their non-radiative relaxation releases heat enabling photothermal energy conversion. (b) Solar irradiance spectrum overlaid with the absorption spectra of exfoliated graphite on a porous carbon foam (red), N-doped porous graphene (blue) and reduced graphene oxide aerogel (green). Insets depict the schematic (red and green) and SEM morphology (blue). Scale bar, 5 μm.[30] Reprinted with permission from ref. 29. Copyright 2018 Nature Energy. (c) UV-Vis spectrum and fluorescence emission profile of CDs under 808 nm laser excitation. Reprinted with permission from ref. 31. Copyright 2019 the American Chemical Society. (d) Solar steam generation using the Janus polypyrrole (PPy) nanobelt@PVA hydrogel evaporator. (i) Schematic representing the fabrication process. (ii) 3D representation of the Janus PPy nanobelt@PVA hydrogel evaporator. (iii) PPy nanobelts as the solar absorbing material on the PVA hydrogel. (iv) Schematic of the 3D water transport through the hydrophilic PPy nanobelts. Reprinted with permission from ref. 56. Copyright 2021 American Chemical Society. (e) Schematic of the core–shell structured hydrogel solar evaporator incorporating MXene/PDA as the photothermal agent. Reprinted with permission from ref. 64. Copyright 2022. Elsevier Ltd. (f) Scheme of the sandwich hydrogel with plasmonic Cu/carbon cells as solar absorbers for solar vapor generation. Reprinted with permission from ref. 69. Copyright 2021 the Royal Society of Chemistry.

compared with the absorption profiles of respective carbon-based solar absorbers composed of an exfoliated graphite layer supported by porous carbon foam (red), N-doped porous graphene (blue) and reduced graphene oxide aerogels (green). These materials depict strong and broad absorptivity. The insets further represent their structural characteristics, schematic of graphite foam and graphene architectures alongside the SEM image of the N-doped graphene.[29,30]

Fig. 2c signifies the optical absorption and fluorescence emission of CDs outlining their best suitability for photothermal applications. The UV-vis absorption spectrum (blue curve) depicts a strong absorption in the UV region around 400–800 nm attributing to π–π* transitions of sp^2-hybridized carbon domains (C=C). The gradual decay in absorption intensity that extends into the visible and NIR region represents the presence of n–π* transitions associated with surface functional groups. This broad, tailing absorption curve confirms their broadband light absorption capacity, which is extremely critical for effective photothermal activity, while the fluorescence emission spectra (red curve) under 808 nm laser excitation show a prominent emission band in the NIR region from 900 to 1200 nm with a peak at 925 nm. It originates from surface defect states and energy traps where excited electrons undergo radiative relaxation followed by non-radiative energy redistribution. It also highlights their excitation-dependent photoluminescence driven by heterogeneity in particle size, surface states and functional groups. The co-existence of the broad absorptivity and NIR emission indicates that a significant portion of absorbed photon energy is dissipated *via* electron–phonon interactions resulting in efficient heat generation. This balance between radiative (fluorescence) and non-radiative decay showcases the significant light-to-heat conversion efficacy, making them a preferable choice as solar absorbers for solar steam generation.[31]

CDs are zero-dimensional carbon nanoparticles whose nitrogen- and oxygen-rich surface functionalities confer strong photoluminescence, chemical stability, biocompatibility, facile functionalization and non-cytotoxicity.[32] They are readily synthesized from natural carbon precursors and distinguished by tunable physiochemical characteristics, aqueous solubility and photostability.[33] Photoexcitation promotes loosely bound electrons to higher states that leads to either radiative or non-radiative relaxation,[34] as already discussed above. The relative partitioning of these channels control light-to-thermal conversion activity,[35] establishing CDs as efficient alternatives to polymeric photothermal nanomaterials.[36] As compared to single-walled carbon nanotubes, CDs offer greater surface area and adsorption sites.[37] Their dispersion within hydrogel matrices prevents aggregation and boosts adsorption,[38] therefore enabling diverse range of applications as in solar energy harvesting,[39] photocatalysis,[40] optical sensing,[41] bioimaging,[42] anticounterfeiting,[43] biomedical studies,[44] supercapacitors[45] and light-emitting devices.

2.1.2. Conjugated polymers. Conjugated polymers, characterized by the sp^2-hybridized carbon[46] backbone, exhibit tunable bandgaps and strong near-infrared absorption,[47] rendering them highly promising for photothermal conversion. Prominent examples such as polypyrrole (PPy),[48–50] polyaniline (PANI)[51,52] and polydopamine (PDA)[53–55] have been extensively employed in solar evaporation systems. Inspired by PPy-based conical solar-absorbing architectures, Zhao *et al.*[56] engineered conical PPy nanobelts prepared by polymerization within the FeOCl template integrated with a PVA hydrogel evaporator by loading the solar absorber directly above the hydrogel {Fig. 2d(i) and (ii)}. It exhibited a solar absorptivity of 98.3% with a solar thermal efficacy of 82.5% along with fast water transport to the evaporation surface {Fig. 2d(iii) and (iv)}, achieving an evaporation rate of 2.64 kg m^{-2} h^{-1} and a photothermal conversion efficacy of 96.3%. Furthermore, the resulting Janus PPy nanobelt@PVA hydrogel demonstrated exceptional desalination performance (99.9%) and a COD removal efficiency of 95.8%. Sustained long-term operation of such evaporators necessitates not only high desalination efficiency but also robust salt resistance.

2.1.3. Semiconductors. Semiconductors are integral to modern industry due to their temperature-dependent resistance[57] and their ability to convert radiant energy into heat *via* photoinduced electron–hole generation followed by non-radiative relaxation.[58] Consequently, they serve as potent photothermal transducers in solar steam systems with widely used materials including MXenes ($Ti_3C_2T_x$ where M is an early transition metal and x is carbon or nitrogen[59]) and metal oxides of titanium,[60] copper,[61] tungsten[62] and molybdenum.[63] Pi *et al.*[64] fabricated a core–shell hydrogel evaporator using MXene/polydopamine (PDA) as a photothermal agent (Fig. 2e), where the HAPAM hydrogel facilitates rapid heat absorption and bulk water transport and the shell exhibits high photothermal efficiency of 94.7% and an evaporation rate of 3.02 kg m^{-2} h^{-1} under one sun irradiation. The presence of aromatic rings and amino groups in PDA imparts effective resistance to heavy metal ions *via* hydrogen bonding and chelation, ensuring durability. Beyond MXenes, metal oxide semiconductors[65] are extensively employed in photothermal evaporation systems.

2.1.4. Metal nanoparticles. Metallic nanomaterials such as silver,[66] copper[67] and gold[68] function as photothermal agents *via* the localized surface plasmon resonance (LSPR) effect, wherein incident light induces collective oscillation of free electrons. The subsequent damping of these oscillations converts kinetic energy into thermal energy, elevating the material's temperature and enabling heat transfer to the surrounding medium. Tian *et al.*[69] developed a sandwich structured PVA hydrogel evaporator integrated with plasmonic Cu and carbon cells (Fig. 2f). Despite incorporating only 50% photothermal material, efficient heat generation arose from electron transfer and internal stress between Cu nanoparticles and carbon matrices, yielding an efficiency of 93.43% and an evaporation rate of 2.08 kg m^{-2} h^{-1}. Additionally, the system demonstrated effective removal of heavy metal ions, indicating significant purification capability.

Moreover, porous substrates such as aerogels,[70,71] hydrogels,[72] wood[73] and foams[74] critically influence the

evaporator performance. Among all the classifications discussed above, CD-integrated hydrogels have emerged as a promising platform, although comprehensive analysis of their aqueous states, morphological design and structural configurations remains limited. This review addresses these gaps providing systemic insights and fundamental guidance for real-world applications.

2.2. Engineering the evaporation surface

Evaporation is enhanced when water spreads into a thin film, increasing the water–air interfacial area; however, the precise regulation of liquid–air interfaces on the micro- and nanoscale remains challenging. Hydrogels offer a promising solution as their surface topography and wettability can be readily engineered enabling controlled evaporation at the hydrogel–air interface.[75] The regulation of surface topography *via* template-assisted synthesis has been shown to significantly enhance evaporation performance with gelation occurring at solid (glass), gas (air) and liquid (pentanol) interfaces. This process yields distinct morphologies – flat (F-SH), grooved (G-SH) and dimpled (D-SH) hydrogels, each exhibiting unique surface architectures. SEM analysis reveals that while F-SH and G-SH possess relatively simple sheet-like structures, D-SH exhibits a hierarchically organized topology with nanoscale pores embedded within microscale cavities. Optical profilometry revealed that hydrated hydrogels with nanoscale surface roughness exhibit a 4.5-fold increase, leading to a 45% higher evaporation rate from F-SH to D-SH due to enhanced surface area, heat flux and water redistribution. Beyond physical surface structuring, the wettability of hydrogel evaporators was chemically tailored to enhance the efficacy.[76] While conventional systems exhibit uniform hydrophilic or hydrophobic character, post-treatment with trichloro(octadecyl)silane (OTS) enabled the formation of hydrophobic patches on a hydrophilic surface. This heterogeneous design enhances evaporation by balancing efficient water transport with reduced salt fouling. X-ray photoelectron spectroscopy and atomic force microscopy confirmed patchy OTS coverage with 30% hydrophobic domains, yielding the highest evaporation rate (4.0 kg m^{-2} h^{-1}) compared to fully hydrophilic and hydrophobic surfaces. This enhancement arises from the confinement of water within hydrophilic regions, leading to reduced surface interaction for outer molecules and additional evaporation at hydrophilic–hydrophobic interfaces. Molecular dynamics simulations corroborated these mechanisms, aligning closely with experimental observations.[77]

2.3. Structure for evaporation

Localization of solar-thermal heat generation to the air/liquid interface is vital for better evaporation performance and high solar-to-vapour energy conversion efficacy. A go-to solution for achieving interfacial heating is the floating of the solar absorber at the air/liquid interface (Fig. 3a) either through surface

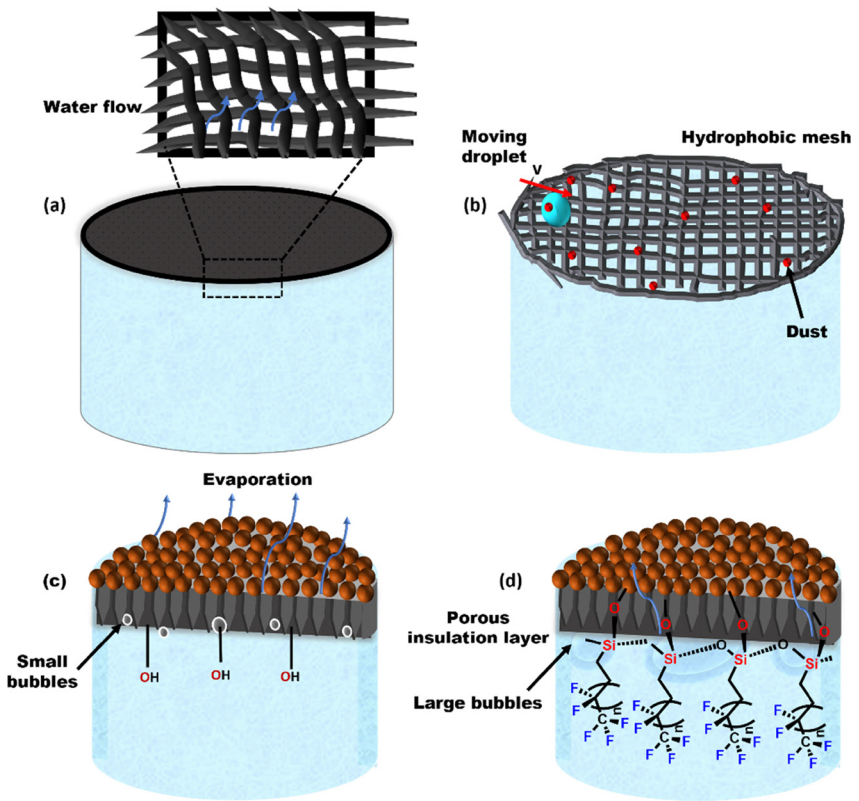

Fig. 3 (a) Schematic of a porous floating structure engineered to localize solar-thermal heating at the water–air interface. (b) Self-cleaning superhydrophobic surface showing droplet motion (V) across the solar absorber. Influence of surface wettability on interfacial evaporation: (c) hydrophilic and (d) fluorosilane-modified hydrophobic bottom layers.

hydrophobicity, low density, or the usage of buoyant, porous materials.[78] Efficient interfacial evaporation requires effective water transport to the heating region, which is enhanced by micrometre-sized pores and good wettability of wicking materials.[79] Light management such as scattering from polystyrene spheres combined with absorbers like Au nanoparticles improves heat localization and evaporation rates. Additionally, surface wettability influences performance where hydrophobic materials can help position light absorbers at the air–water interface.[80] Inspired by this, Liu *et al.*[81] reported that superhydrophobic carbon-coated gauze offers lotus-leaf like self-cleaning (Fig. 3b), durability and efficient evaporation with reduced contamination. Hydrophilic surfaces enhance water wicking and capillary pumping (Fig. 3c), while a hydrophobic AAO bottom layer (Fig. 3d) lowers wettability, reducing heat transfer and efficiency.

In 2023, Gui *et al.*[82] designed hierarchical evaporators comprising hydrogel layers and ice-templated aerogel substrates with natural materials compatible with photothermal conversion (PTC) materials. Owing to this, local dual-layered structures and vertically aligned channels were set up, which guaranteed structural integrity and adequate transportation of water during evaporation. More recently, in 2025, Liu *et al.*[81] developed porous glass evaporators (PGEs) that have a blend of glass powders with soluble salts providing continuous pores. The microstructure of the evaporator consisted of micrometer-scale pores with interconnected porous channels. PGE demonstrated an evaporation efficiency of 98% achieving a rate of 2.21 kg m^{-2} h^{-1} in pure water. Comparatively, in seawater and methylene blue solution, the evaporation rates exhibited were 2.08 and 2.47 kg m^{-2} h^{-1}. In addition, in altered acidic and alkaline treatments, the rates retained were 2.0 kg m^{-2} h^{-1}. The prevention of salt deposition and structured water transport with robustness and dominant water evaporation performance are considered to be remarkable advances in solar water evaporators.

2.4. Reduction of evaporation enthalpy

Polymer chains within hydrogels exhibit strong affinity for water molecules, giving rise to distinct hydration states. Water molecules that strongly interact with polymer functional groups on the hydrogel matrix are classified as bound water (BW), whereas bulk liquid behaves as free water (FW) with negligible interactions. In between the bound water and free water, there exists the intermediate water (IW), which is weakly coordinated to both the polymer network and the neighboring water molecules, and therefore, it requires less energy to vaporize.[83] Enriching the hydrogel with IW consequently lowers the energy demand, further amplifying the evaporation rate and efficiency. The Hofmeister effect plays a pivotal role in modulating interfacial hydration, where salt ions restructure water molecule's hydrogen bonding to accelerate IW formation. Ions are classified as kosmotropes which enhance the hydrogen bonding, resulting in proper arrangement of water molecules, thus leading to the formation of IW. Hydrophilic functional groups, such as hydroxyl (–OH), amide (–CONH–), amino ($–NH_2$), sulfonic acid ($–SO_3H$), and carboxyl (–COOH), stabilize IW through non-covalent interactions.[84] Leveraging these tunable polymer–water interactions, a PVA-based hydrogel incorporating polypyrrole (PPy) as the photothermal agent was developed. The hydroxyl groups of PVA promote IW formation by weakening intermolecular hydrogen bonding and reducing the evaporation enthalpy, while PPy converts incident sunlight into localized heat. Simultaneously, branched micron-scale channels and internal gaps facilitate rapid water diffusion and capillary pumping, ensuring a continuous supply to the evaporative surface[85] (Fig. 4a).

Characterization techniques such as differential scanning calorimetry (DSC), infrared spectroscopy, Raman spectroscopy, and nuclear magnetic resonance have been employed to probe water states within hydrogels. Reported findings demonstrate that the distribution of BW, IW and FW can be modulated by hydrogel constituents – polymer concentration, crosslinking density, functional fillers and the network's porosity (Fig. 4b).[76,86] An interpenetrating polystyrenesulfonate (PSS) and PVA hydrogel was developed by immersing pre-crosslinked and freeze-dried PVA into a sodium styrenesulfonate precursor, producing a network hydrated through both electrostatic interactions and hydrogen bonding (Fig. 4c). DSC analysis differentiates the unique water states by identifying exothermic and endothermic peaks during cooling and melting, the two melting peaks corresponding to FW and IW. The results showed that PSS increases bound-water content, reflecting stronger electrostatic polymer–water interactions, also elevating the free-water fraction. An optimal PSS/PVA ratio of $\sim$ 1.5 : 1 maximizes the intermediate to free water ratio and lowers the effective evaporation enthalpy by approximately 50% and demonstrated an enhanced evaporation rate of 3.9 kg m^{-2} h^{-1} (Fig. 4d), indicating that molecular and mesh-scale compositional tuning can potentially lower the evaporation enthalpy.[87] This efficient strategy has been extended to numerous other solar vapor-generation systems using diverse material combinations and designs. It can be quantified using the following equation:

$$\Delta H_{eq} = \frac{\dot{m}_0 \times \Delta H_{vap}}{\dot{m}_g}$$

where ΔH_{eq} is the equivalent evaporation enthalpy of the hydrogel, $\dot{m}_0$ is the evaporation rate of bulk water, ΔH_{vap} is the evaporation enthalpy of bulk water at a specific temperature and $\dot{m}_g$ is the mass change of the hydrogel.[88] Recently, Li *et al.*[89] have prepared a $Ti_3C_2T_x$/CuO photothermal heterojunction by electrostatic adsorption and incorporated it into a chitosan (CS)/polyacrylic acid (PAA) hydrogel. The hydrogel backbone enriched with hydrophilic groups increased the fraction of intermediate water, lowering the evaporation enthalpy to 940.8 J g^{-1} which yielded 3.14 kg m^{-2} h^{-1} (86% energy efficiency) in 1 wt% saline and 2.56 kg m^{-2} h^{-1} in 10 wt% brine, as confirmed by the DSC measurements. Raman spectroscopy and density functional theory (DFT) results indicated a weakened hydrogen bonding between intermediate water and polymer chains, reducing the vaporization energy barrier. This

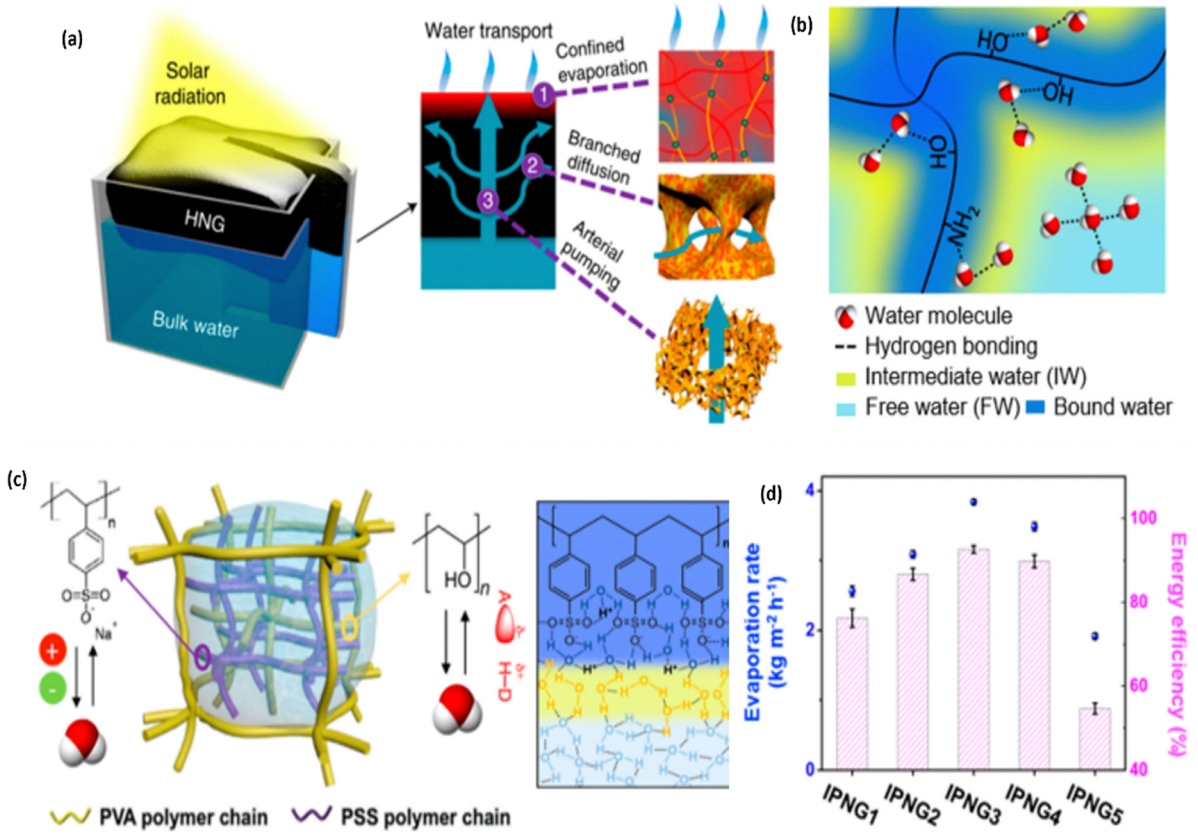

Fig. 4 (a) Schematic of the hydrogel-based solar vapor generator with capillary-driven water transport. (b) Representation of polymer–water hydrogen bonding, weakened water–water interactions and normal bulk water bonding. (c) Illustration of the interpenetrating hydrogel showing the PSS network's electrostatic and hydrogen-bonding interactions with water. (d) Evaporation rates and energy efficiencies of IPNGs under 1 sun illumination; IPNG1–IPNG5 represent PSS : PVA ratios of 0 : 1, 1 : 1, 1.5 : 1, 2 : 1 and 1 : 0. Reprinted with permission from ref. 76. Copyright 2021 the American Chemical Society.

novel work shows that tailoring hydrogel water states, basically elevating the intermediate water proportion *via* hydrophilic chemistry combined with photothermal integration can be an effective route to lower the evaporation enthalpy and boost the evaporation rate.

2.5. Heat distribution management

Solar steam generation technologies achieve reduced heat loss, enhanced energy conversion efficiency and improved freshwater yield through optimized heating strategies. In bottom heating, light-absorbing materials are positioned at the base suffering from significant thermal losses due to spatial separation between the heat source and evaporation interface, thereby limiting the overall efficacy. Volumetric heating addresses this by dispersing photothermal nanoparticles within the water enabling bulk heating and rapid vaporization, although issues related to nanofluid stability and aggregation hinder long-term applicability. In contrast, interfacial heating localizes light-to-heat conversion at the air–water interface, where absorbed solar energy generates a confined high-temperature region that accelerates the evaporation efficiency and aids in effective separation of water from dissolved impurities, thereby establishing it as the most advantageous and viable approach among the three strategies. The tunable structure and *in situ* integration of photothermal materials ensure balanced water transport and efficient heat distribution for improved evaporation.[80,85,90,91]

2.6. Designing of the thermal insulation

Proper designing of the thermal insulation is essential for heat localization at the air/liquid evaporative interface, lessening the loss of heat and improvising the evaporation efficacy. The downward conduction loss (q_{water}) is dependent on the thermal conductivity of the insulator (k) and can be estimated by $q_{water} = -kA\mathrm{d}T/\mathrm{d}x$, where A refers to the surface area of the solar absorber facing the sun and $\mathrm{d}T/\mathrm{d}x$ refers to the temperature gradient from the solar absorber to water.[92] In terms of the measured temperature of evaporation interface, the upward convection and radiation loss can be calculated theoretically. To minimize the downward conductive heat loss in one-layered designs (Fig. 5a), a porous carbon foam thermal insulation layer (with air filled closed pores) is used beneath the solar absorber, in two-layer designs[93] (Fig. 5b). In one reported implementation, a closed-cell polystyrene foam served as the insulator and was overlaid with hydrophilic cellulose, which pumps water to the heated surface *via* capillary wicking, therefore maintaining a continuous thin wet layer for better interfacial evaporation (Fig. 5c and d). An effective evaporation

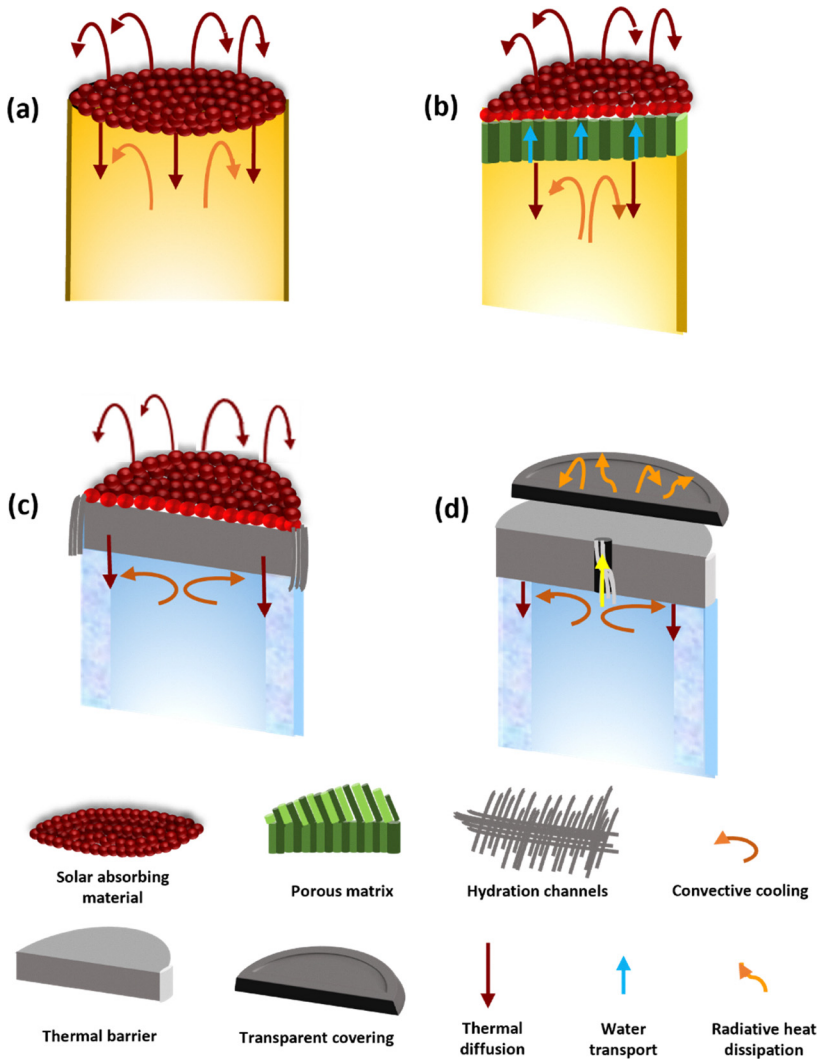

Fig. 5 (a) Schematic of a single-layered floating evaporation structure designed for efficient solar-driven water evaporation. (b) Double-layer floating structure with porous thermal insulation for efficient solar evaporation. (c) Double-layer design featuring a closed pore thermal insulator for reduced downward heat loss. (d) Reduction of radiative and convective heat losses from the top solar-thermal surface using a selective absorber and a transparent bubble wrap cover.

structure should possess both low thermal emittance and high thermal reflectance at the wavelengths where water emits thermal radiation.[94]

In 2022, Chen *et al.*[95] reported a combination of solar selective absorber and passive radiative cooling techniques achieving high solar thermal conversion efficiency η_{evap} = 0.894 at 1 sun, high solar reflectance = 0.927 and thermal emittance = 0.929. It enhances solar thermal conversion efficiency, thereby reducing thermal radiation loss. In 2023, Wang *et al.*[96] designed a Janus evaporator having an appreciable rate of evaporation, *i.e.* 1.707 kg m^{-2} h^{-1} under 1 sun irradiation, remarkably with complete salt elimination during continuous desalination of 15 wt% and 3.5 wt% simulated seawater for 15 cycles (7 h each cycle). Low emissivity absorber was used as a coating on the aluminium sheet for photothermal conversion, directly averting salt deposition on the solar absorber, as low emissivity reduces heat loss enabling systematic solar utilization. This steam generator effectively facilitates solar energy collection and water evaporation without any salt accumulation even at higher concentrations. In 2024, Jiang *et al.*[97] developed a biomass-based salt-resistant 3D evaporator constituting bamboo leaf-derived carbon (BLC) and heat-insulating macroporous melamine foam (MF), exhibiting multi-beneficial solar vapor generation performances. The BLC/MF evaporator is incorporated with good thermal conversion of light having an evaporation rate surging to 2.29 kg m^{-2} h^{-1} and an appreciable evaporation efficiency of 93.95% under the light intensity of 1 kW m^{-2}. The evaporator's versatile design and low thermal conductivity ensure high-performance water purification that meets the drinking standards recommended by the WHO. Furthermore, its structural stability and ability to prevent salt accumulation make it highly effective for consistent, long-term use in portable outdoor desalination.

3. Carbon dots in solar water evaporation

3.1. Photothermal properties of carbon dots

Carbon dots (CDs), well-known for their remarkable light absorbing properties and efficient electron transport abilities, can expand the light response range of photocatalysts.[98] CDs have gained much attention for their efficacy in modifying photocatalysts. Biomass-derived CDs, specifically those synthesized from peanut shells provide varied advantages including widespread availability, cost-effectiveness and environmental benefits.[99] In conventional photothermal therapy, the generation of heat is caused by localized surface plasmonic resonance (LSPR) of metallic nanoparticles, typically composed of gold and silver. The insufficiency of biological tolerance of metallic nanoparticles has led to the emergence of biocompatible, multifunctional, environmentally benign and functionally superior alternatives.[100] In recent times, photothermal transduction agents have been utilized for solar steam generation. Amongst the accessible photothermal agents for photothermal conversion, carbon dots (CDs) offer boosted photothermal conversion efficiency (PCE) and broad absorption spectra, while their lower heat conduction minimizes heat dissipation and promotes efficient localized heat generation.[101] The purification of contaminated water is achieved through adsorption into a porous medium infused with carbon dots (CDs), followed by evaporation driven by the heat generated from the photothermal effect of the CDs.[102] It has been illustrated that the on-site self-assembly of CDs on the surface of processed wood can lead to photothermal conversion characterized by increased permeability and highly accessible oxygen-containing functional groups (*e.g.*, hydroxyl groups), which are considered to enhance the solar evaporation efficacy.[103,104] Hydrogels being porous materials exhibit a large surface area and abundant active sites, both of which are benefiting for the augmentation of the photocatalysts' capability to absorb light and enhance the catalytic activity. By the combination of these materials, it is now possible to develop photocatalysts with better catalytic efficiency and appreciable stability, making them highly apt for real-life applications.[105]

3.2. Carbon dot-based solar water evaporators

With growing scopes of solar steam generation, solar evaporators are typically designed with a two-layer configuration, where the top layer consists of porous photothermal materials and the bottom layer functions as a thermally insulating float. The permeable photothermal layer generally comprises carbonaceous agents such as multilayer graphene, carbon nanotubes, carbonized polymers, carbonized wood, and graphite due to their broadband light absorption, high photothermal conversion efficiency, photostability, biodegradability, and low toxicity.[106] However, these carbon materials generally exhibit high thermal conductivity, which leads to undesirable heat emission from the top layer. Thus, there remains a necessity for carbon-based materials that combine efficient solar thermal conversion capacity with lesser heat transfer capability. Encapsulated CDs enable the preparation of a robust and recyclable nanocomposite designed for structured solar vapor generation and salt elimination from water.[107] In 2023, Rahmawati *et al.*[108] reported an excellent evaporation efficacy of 70% exhibiting a vaporization rate of 1.11 kg m^{-2} h^{-1} under illumination at 1 kW m^{-2} by utilizing CDs as photothermal materials in the solar evaporator, thereby enhancing their durability and stability as well as paving the way to design and functionalize CDs in solar water evaporators for efficient optical and photothermal properties. Carbon dots play the role of primary photothermal agents in the system, facilitating the conversion of sun's radiation into heat that elevates the temperature of the water absorbed within the hydrogel, thereby inducing evaporation followed by the recondensation of purified water. Moreover, the CDs improve the structural integrity of the hydrogel *via* cross-linking interactions between their surface functional groups and hydrogel matrix. As a whole, it can be concluded that the CD-oriented hydrogel led to the appreciable desalination, decontamination of water carrying heavy metal ions, detergents or organic dyes. The CD/hydrogel composite demonstrated visibly advantageous applicability: recycling ability, ease of fabrication, and the use of less expensive, eco-friendly and easily accessible components. This technology can be practically utilized in sustainable and cost-effective water desalination platforms or portable water purification devices (Fig. 6). In 2020, Wang *et al.*[109] developed a novel CD-based solar evaporator by incorporating nano-sized CDs on microporous substrates (Fig. 7) exhibiting an evaporation performance of 2.31 kg m^{-2} h^{-1} under one sun illumination along with a prominent deformation tolerance due to the strong interfacial adhesion between the CDs and cellulose. Its salient mechanical properties contributed to its high evaporation rate of 2.93 kg m^{-2} h^{-1}.

In 2022, Tian *et al.*[110] constructed a biomimetic and biomass-derived solar evaporator with a combination of agar and titanium nitride nanoparticles (Fig. 8a) with excellent photothermal conversion efficiency that facilitated a solar absorptance of 0.98. This convenient device comprised vertically aligned channels further fabricated with an ice template-induced self-assembly forming a wood-like structure. This enhanced its evaporation rate up to 5.15 kg m^{-2} h^{-1} in pure water and 4.5 kg m^{-2} h^{-1} in 3.5 wt% saline water (Fig. 8b), also offering good recyclability, utilization of economical materials, better desalination outcomes and superior quality freshwater yields. The design of evaporators with remarkable heat management and minimised heat loss with the view of achieving better evaporation efficiency still remained a stumbling block, based on this, in 2023, Zhang *et al.*[111] designed a mushroom-structured hydrogel evaporator consisting of the fabrication of biomass lotus root starch (LR), polyvinyl alcohol (PVA) and ink-modified carbon quantum dots and TiO_2 (i-CQDs–TiO_2) (Fig. 8c), demonstrating the rate of evaporation as 3.78 kg m^{-2} h^{-1} with an efficacy of 98% (Fig. 8d). The main highlight of the work is its outstanding salt resistance (Fig. 8e), where the evaporation rate was noticed to remain consistent even at high pH and salinity ranges. CDs appreciably boosted

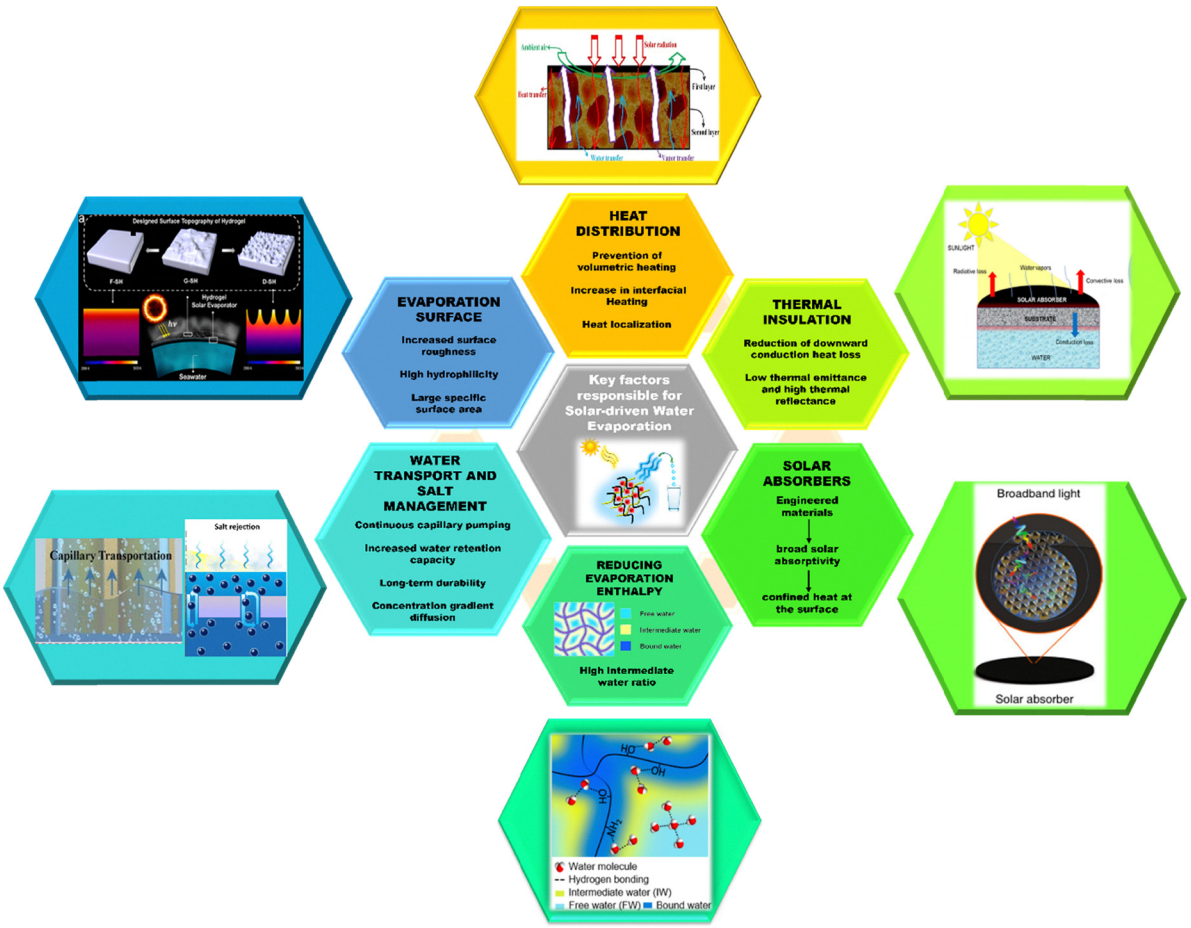

Fig. 6 Comprehensive figure summarizing the key factors responsible for solar-driven water evaporation.

the mechanical and photothermal conversion capability for solar vapor generation. With specific emphasis on carbon dots employed in solar evaporators and their sources, in 2025, He *et al.*[112] produced a distinctive photothermal material comprising carbon dots for which the carbon source was extracted from the leaves of *Rhus typhina* L. combining them with carbon black and further depositing them on basalt fabric (Fig. 8f). It was found that the novel material exhibited a good light absorption capacity, notably a low evaporation enthalpy of 1681 J g^{-1} with the rate of evaporation as 2.05 kg m^{-2} h^{-1} in water and an elevating light-to-heat conversion efficiency of 95.72% under 1 sun irradiation (Fig. 8g). This proved to be a sustainable solution for the preparation of photothermal materials used in solar steam generation technologies.

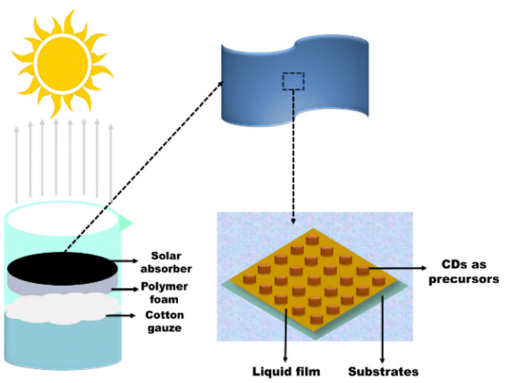

Fig. 7 Schematic of steam generation.[109]

4. Hydrogels in solar water evaporation

4.1. Properties of hydrogels

Hydrogels have emerged as pioneering materials for solar-driven vapor generation owing to their advantageous attributes comprising high swelling capacity, superior optical transmittance, thermal robustness, intrinsic porosity, structural flexibility and cost-effectiveness. Leveraging these characteristics, hydrogels offer a sustainable and efficient platform for augmenting vapor generation and facilitating the generation of cleaner water.[113] Composed of hydrophilic polymer networks with both solid- and liquid-like characteristics,[114] they provide diverse interaction sites and have broad applications in biomedicine,[115] wearable electronics[116] and environmental remediation.[117] Despite their inherently limited porosity, the performance can be enhanced through techniques such as salt

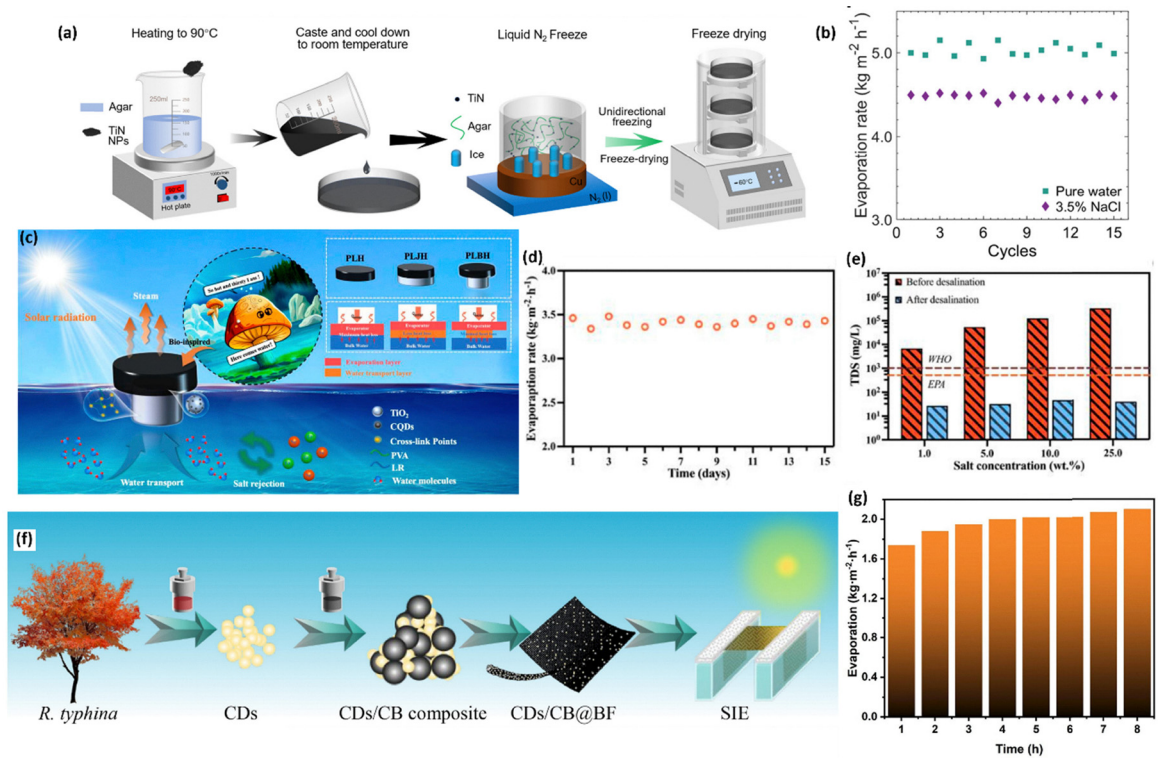

Fig. 8 (a) Agar and TiN hydrogel-based evaporators (ATHEs) prepared by ice-template-induced self-assembly and subsequent freeze-drying. (b) ATHE continuous stability for 15 h (1 h cycle each). Reprinted with permission from ref. 110. Copyright 2022. Elsevier B.V. (c) Schematic of the PLBH evaporator for seawater desalination. (d) Evaporation stability of the evaporator over 15 days (e) comparison of the amount of TDS in water before and after desalination across four different salt concentrations. Reprinted with permission from ref. 111. Copyright 2023 Elsevier B.V. (f) Schematic representing the CDs/carbon black@basalt fabric (CDs/CB@BF) evaporator with *Rhus typhina* L. as the carbon source (g) evaporation rates of CDs/CB@BF over 8 h. Reprinted with permission from ref. 112. Copyright 2025 Elsevier B.V.

leaching and pore formation, although with increased fabrication complexity. They prove to be significantly advantageous from both the fundamental view and real-life view for solar-enabled water purification technologies[118] and renewable energy generation (Fig. 9).

Innovative hydrogels are mostly used in water purification owing to their larger surface area, strong temperature withstanding ability, better selectivity, and lesser external energy consumption. Among all, thermosensitive and photo-responsive innovative hydrogels have the peculiar feature of responsiveness to environmental stimuli, laying a vital base for advanced water treatment. Advanced materials respond to the energy from the sun's rays, thereby achieving switching effects bringing a change in their inner structure and characteristics. Therein, researchers continue to explore innovative hydrogel-based solar steam generation systems to fulfil the rising need for inexhaustible energy resources (Fig. 10).[119]

4.2. Photothermal hydrogels for solar water evaporation

Hydrogel composites act as tunable hosts with adjustable photothermal characteristics, which can be harnessed as solar evaporators governed by the nature and concentration of the solar absorber used and the design of a well-structured polymeric network. Their permeable 3D interpenetrating framework facilitates the formation and mobility of weakly bound water molecules[120] through tailored polymer–water interactions, enhancing transport dynamics. Additionally, optimized surface parameters and uniform dispersion of photothermal absorbers within the porous matrix maximize solar absorption and heat localization, thereby minimizing thermal losses and accelerating evaporation. Radiative losses can be minimized through the use of low-emissivity materials or by controlling the surface temperature. A required criterion for maximizing the efficacy of solar evaporators is to precisely choose polymers with high water affinity and implement a well-structured design of the framework to incorporate materials with remarkable light-to-heat conversion capacity into hydrophilic polymeric strands.[121]

In 2022, Li *et al.*[122] prepared a full-polymer salt-tolerant anionic photo-electrolyte-based hydrogel as an "all-in-all" evaporator, providing both photothermal as well as electrostatic repulsion properties. The material had a 3D reticular porous structure exhibiting a solar absorption efficiency of 95.5% in 380–2500 nm and an evaporation enthalpy lowered to 1624.14 kJ kg^{-1}. Irradiating with simulated sunlight of 1.0 kW m^{-2}, it produced a good evaporation rate of 2.5 kg m^{-2} h^{-1}. Basically, the hydrogel comprised poly(vinyl alcohol) forming the skeletal arrangement and poly(3,4-ethylenedioxythiophene) (PEDOT) and poly(sodium-*p*-styrenesulfonate) (PSS) as solar absorbers, also possessing hydrophilicity and negative charges (Fig. 11a).

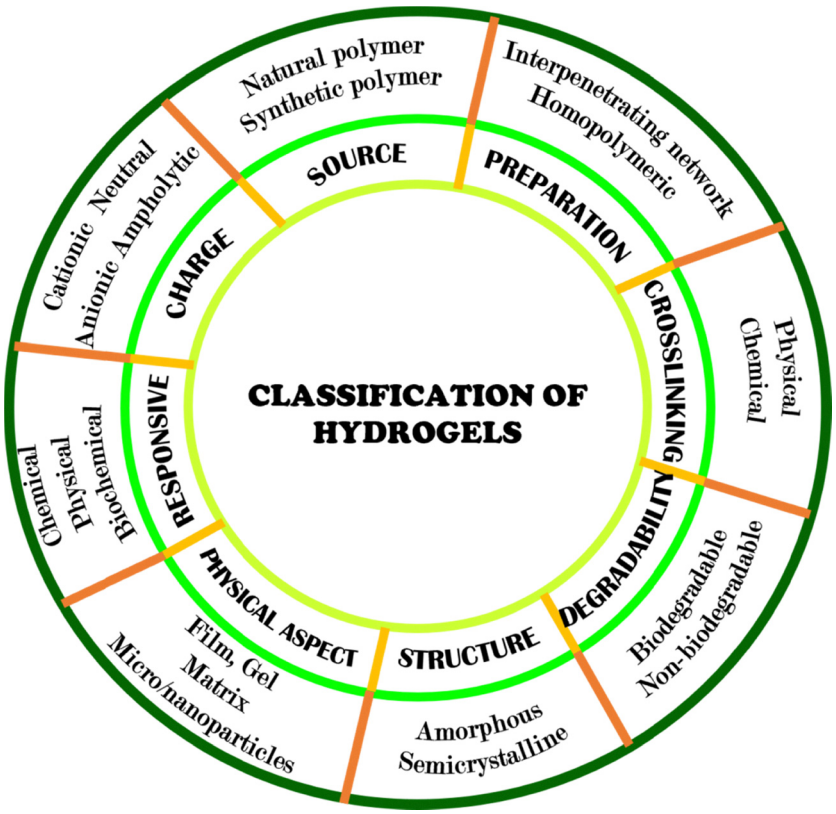

Fig. 9 Comprehensive classification of hydrogels based on structural composition, crosslinking mechanism, origin, and responsiveness.

Moreover, –OH and SO_3^- facilitate the interaction between the hydrogel and water molecules, leading to low evaporation enthalpy and specifically, the negatively charged SO_3^- isolates Na^+ from Cl^- through an electrostatic repulsion effect, thereby attaining excellent salt-resistant behaviour and better evaporative robustness. For a further initiative towards sustainability, in 2023, Ni *et al.*[123] developed a photothermal hydrogel evaporator through a blending pathway constituting eco-friendly poly(vinyl alcohol), agarose, Fe^{3+} and tannic acid, where the TA*Fe^{3+} complexes being the photothermal agents (Fig. 11b) provided remarkable gelatinization ability and light-absorbing properties, attaining a better evaporation rate of 1.897 ± 0.11 kg m^{-2} h^{-1} with a better energy conversion efficacy of 89.7% ± 2.73%. In 2024, Liu *et al.*[124] devised a thermos-responsive hydrogel evaporator employing 3D printing technology and inculcating hydrophilicity/hydrophobicity phase transition (Fig. 11c) to enhance water transport stability obtaining an evaporation rate of 3.587 kg m^{-2} h^{-1} and an efficiency of 95.3% (Fig. 11d) along with better photo-thermal conversion, excellent thermal conductivity, and specifically, antifouling abilities, enhancing its practical utilization. In 2025, Li *et al.*[125] demonstrated that it is crucial to balance the water supply rate and thermal localisation during evaporation. In this view, they designed super-hydrophilic (Ink-MoS_2/PAM/HPC) (IMPH) photothermal hydrogels with vertically aligned channels, providing a tunable aperture and an optimized hydratable polymeric network comprising polyacrylamide/hydroxypropyl cellulose (Fig. 11e) to be utilized as superior-performance interfacial evaporators achieving an evaporation efficiency of 90.0% at a rate of 2.68 kg m^{-2} h^{-1} under a light intensity of 1 kW m^{-2} with appreciable salt-resistance, self-cleaning ability, reduction of evaporation enthalpy and better water transfer and heat management (Fig. 11f). Photothermal 3D hydrogels intensify the rate of evaporation with their solar-induced dual energy supply channels, thereby synergistically managing water transport and energy uptake. In 2025, Huang *et al.*[126] skillfully constructed an integrated solar evaporator with a 3D tree-ring-structured hydrogel, incorporating the chelation of Cu^{2+} with sodium humate (SH) as photothermal agents into the sodium alginate/polyacrylamide (SP/PAM/Cu@SH) (SPCS) hydrogel matrix, optimizing their activity, stability, efficient water transport and salt resistance. This novel strategy displayed a rate of evaporation of 2.23 kg m^{-2} h^{-1} in deionized water, which further exhibited better evaporation performance with a rate of 3.69 kg m^{-2} h^{-1} through the combination of photothermal agents, solar-induced heat field and a concave evaporation surface by placing a photothermal polylactic acid enclosure surrounding the 3D hydrogel (Fig. 11g).

4.3. Advantages of hydrogel-based solar water evaporators

The combination of hydrogels with photothermal materials represent advanced substrate materials for solar steam generators.[127] Hydrogels provide high water affinity, a penetrable framework and a larger surface area that is advantageous for proper water uptake, water-holding capacity and water permeability.[128] The inclusion of hydrogels in solar-

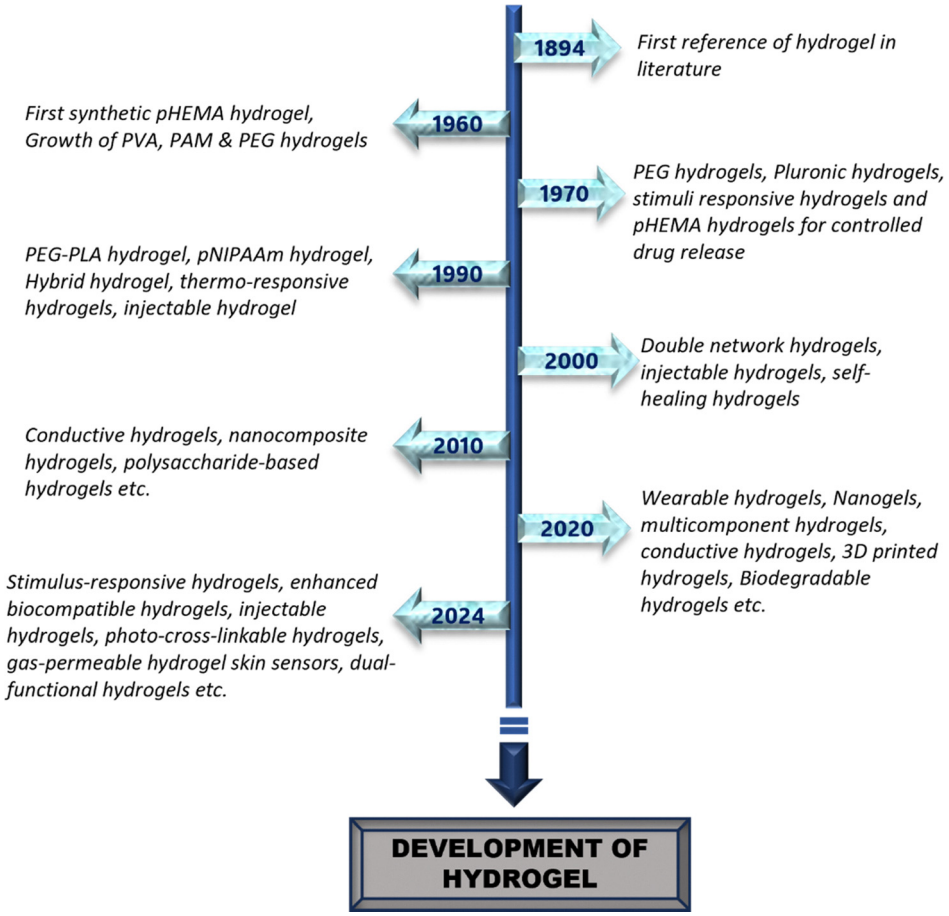

Fig. 10 Chronological overview of the advancements in hydrogel development.

responsive evaporator systems can efficiently modulate water transport and enhance the photothermal conversion efficacy, evaporation efficiency and its rate.[129,130] Hydrogels with pores sufficiently allow the exterior force to disperse and keep the morphological parameters intact and improve the reflection and scattering of internal light with increased capturing of light energy.[131] Moreover, hydrogels have preferable mechanical properties that supervise the change in shapes and reusability in real-life applications.[132] One notable merit of employing them in hydrogel-mediated solar water treatment devices is their adjustable water retention ability and regulated transport dynamics for ensuring sustained water delivery. Along with their easily tunable water transport, these evaporators have an advanced heat localization effect, thereby possessing lesser heat loss at the air–water interface along with low thermal conductivity.[133] Additionally, it confirms stability, recyclability, reusability and salt-tolerance, which reach the adequacy for productive evaporation performance and increased water generation. These above-mentioned merits assure that it consistently transports water to the evaporative surface and facilitates rapid evaporation, therefore exhibiting better energy transformation.

The design of hydrogels with varied functionalities, namely anti-fouling ability, permselectivity and thermal responsiveness, makes the solar evaporators suitable for different applicabilities.[134] The adjustability of the physical and chemical properties facilitate the optimization of the performance of the solar vapor generator. Moreover, there is a flexibility to further enhance salt-resistance, mechanical properties and lessen evaporation enthalpy.[135,136] In addition, several hydrogel materials are the derivatives of natural resources being eco-friendly and provide sustainability, and there is an ease of preparation, requiring lesser energy in comparison to traditional desalination methodologies (Table 2).[137,138] Most of the hydrogel-based solar steam generators can also be flexibly tuned to perform synergistic functions[139,140] (Fig. 12).

As discussed in Table 3, hydrogels exhibit certain key advantages over other evaporation membranes and aerogels, specifically superior water transport to the evaporation surface, active thermal management that lowers the effective energy penalty for vaporization, intrinsic multifunctionality for decontamination and broad design flexibility for tailoring wettability, porosity and surface chemistry. However, the principal drawbacks that persist can be mitigated. The mechanical fragility is readily addressed by reinforcing the polymer matrix with fibrous scaffolds, sponges or cross-linked composites (*e.g.* PVA) to improve toughness and stability. Salt accumulation, under extreme conditions, can be minimized by implementing

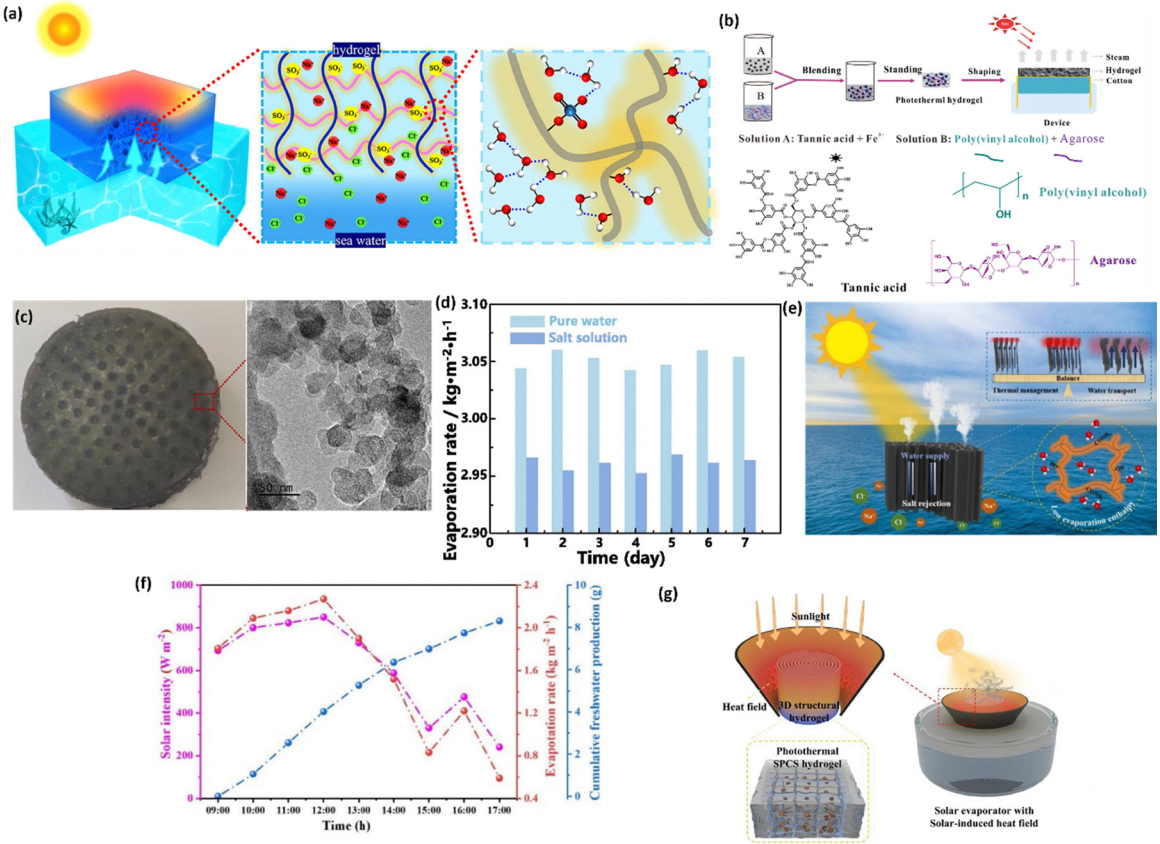

Fig. 11 (a) Diagram of the solar-vapor generator using a salt-tolerant anionic polyelectrolyte hydrogel. Reprinted with permission from ref. 122. Copyright 2021 Elsevier B.V. (b) Schematic illustrating a photothermal hydrogel with a TA*Fe^{3+} complex as the photothermal agent fabricated by a facile blending method. Reprinted with permission from ref. 123. Copyright 2023 Elsevier Inc. (c) Image using the thermo-responsive hydrogel using a 3D printing technology along with the TEM image. Scale bar: 50 nm. (d) Evaporation rate of the 3D thermo-responsive hydrogel in pure and salt solution. Reprinted with permission from ref. 124. Copyright 2024 International Solar Energy Society. Published by Elsevier Ltd. (e) Schematic of the IMPH hydrogel with vertically aligned channels. (f) Evaporation rate of IMPH hydrogel under a solar intensity of 1 kW m^{-2}. Reprinted with permission from ref. 125. Copyright 2025 Elsevier B.V. (g) Illustration of the SPCS hydrogel with solar-induced heat field. Reprinted with permission from ref. 126. Copyright 2025 Elsevier B.V.

vertical channels, salt-rejection surface chemistries or routine flushing strategies to maintain continuous solar evaporation. Concerns about durability and standardization can be resolved by adopting accelerated-aging protocols, standardized performance metrics and life-cycle cost analyses to validate real-world implementations. For applications that require high water flux, integrated contaminant removal and adaptable form factors, especially portable, low-cost or enhanced desalination, hydrogel-based solar vapor generators offer the optimal balance between performance and practicality. Prioritizing composite designs (*i.e.* hydrogel, robust scaffold and photothermal CDs) facilitates retaining the advantages of hydrogels while overcoming the mechanical and longevity constraints.

5. Carbon dots and hydrogel composites in solar water evaporation

5.1. Synergistic effects of carbon dot–hydrogel composites

Often, hydrogel materials suffer from inadequacy in mechanical strength, quenching their applicability. These demerits are attainable synergistically. Particularly, hydrogels serve as a supportive framework that facilitates superior dispersion of CDs while preserving their photoluminescent integrity. Simultaneously, CDs also facilitate reinforcement of the mechanical potency of the polymeric matrices.[145] Moreover, the incorporation of CDs uplifts the hydrogel's thermal stability as a whole, adhesiveness, self-healing ability, and rubber-like elasticity. It is believed that the encapsulation of CDs increases physical crosslinks and non-covalent interactions, as in hydrogen bonding and electrostatic (ES) forces, which consequently improvise the characteristics of the hydrogel.[146] The functional groups present on the surface of CDs play a characteristic role constituting the building block units of the hydrogels. Through the synergistic interplay of non-covalent interactions and covalent bonding, CDs function as the crosslinking centres within the hydrogel polymer networks, resulting in the formation of densely crosslinked hydrogels which integrate with the functional attributes of both CDs and hydrogel matrices. This structural integration enhances the mechanical strength, self-healing ability and adsorption capacity of the CD-incorporated hydrogel composites further along with fluorescence and

Table 2 Summary of natural and synthetic polymers employed in hydrogel fabrication, including their sources, properties, and limitations

Natural polymers	Source	Properties	Limitations
Alginate Agarose Chitosan Collagen Cellulose Fibrin Gelatin Hyaluronic Pectin	Derivatives from plants, animals, microorganisms and algae.	Biocompatibility, biodegradability, biosafety, low immunogenicity, cost-effective and adhesive in nature	Mechanical properties are limited, difficulty in purification and minor immune response due to impurities
Synthetic polymers	**Source**	**Properties**	**Limitation**
PEG [polyethylene] PVA [poly(vinyl alcohol)] PU [polycarbonate urethane] Poly[epsilon-caprolactone] Poly[anhydride] PPF [propylene fumarate] PCL [poly(caprolactone)] PLA [poly(lactic acid)] PLGA [poly(lactic-*co*-glycolic acid)]	Polymerisation of synthetic monomers	Comparatively economical than natural polymers, prolonged shelf-life, efficient delivery of soluble molecules, unreactive, degradation rate can be regulated and high reproducibility	Triggers immune response, inflammation reactions and less biocompatible

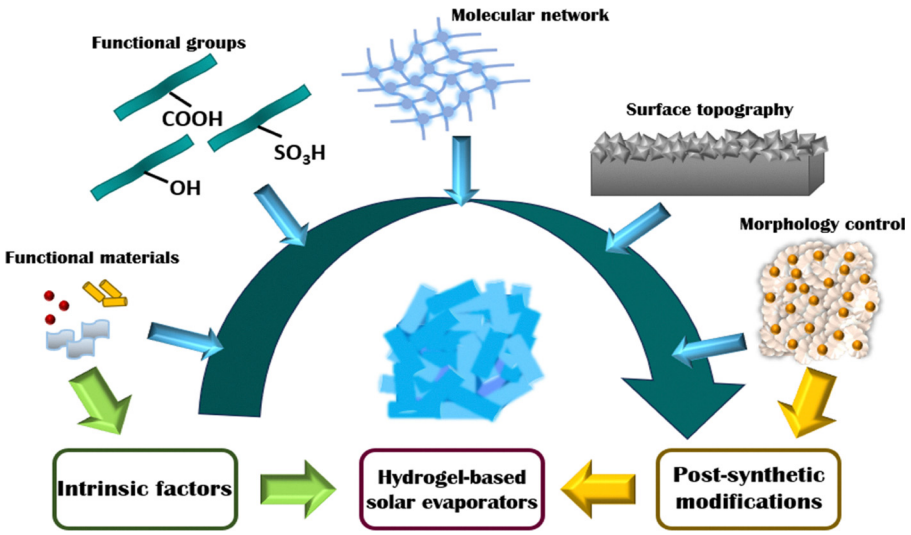

Fig. 12 Design strategies of hydrogel-based solar evaporators for water purification applications.

sensing functions. Considering the higher fluorescence stability of CD-based hydrogels prohibiting the fluorescence aggregation-caused quenching (ACQ) of CDs is efficiently mitigated through their integration into hydrogel matrices. This combination represents a synergistic approach, whereas the hydrogel network prevents CD aggregation, therefore suppressing the ACQ effect and significantly improving fluorescence stability.[147,148] On the other hand, comparing with hydrogels, CD-based hydrogels exhibit strengthened as well as enhanced properties. Therein, the versatile CD-incorporated hydrogel composite fabricated by the integration of CDs and hydrogels show a widened spectrum of applications covering purification, photocatalytic degradation, solar desalination, adsorption, detection, target-responsive behaviour and pH-dependent response (Fig. 13).

Numerous studies have reviewed the synthesis, functional mechanisms and diverse applications of carbon dots and hydrogels individually, but comprehensive reviews particularly addressing CD-integrated hydrogel systems remain limited. Thus, this makes it necessary to bring forward a detailed overview of the relevant applications and development possibilities of CD-based hydrogels.[149] In 2019, Singh *et al.*[150] reported the fabrication of a novel composite consisting of carbon dots (C-dots) enclosed in a permeable hydrogel. The hydrogel system facilitated better absorption of water, wherein the carbon dots provided better thermal and mechanical stability. It exhibited

Table 3 Comparative analysis of hydrogels, traditional evaporation membranes and aerogels based on key characteristics[141–144]

Characteristics	Traditional evaporation membranes/aerogels	Hydrogels	Hydrogels with their advantages
Water transport	Significantly low (in membranes) and comparatively moderate (in aerogels) with tortuous, disordered pores increasing the flow friction	Very high, facilitating continuous capillary pumping	Membranes have mass transfer resistance and cause membrane wetting. Aerogels have a rigid framework that lowers bulk static water retention, whereas hydrogels physically expand and uncoil increasing the water retention and evaporation rate.
Heat management	Moderate (in terms of membranes) and excellent insulation but lesser interfacial control (in terms of aerogels)	Excellent; lowering the effective H_{vap} and maximizing heat localization	In hydrogels, significant interfacial heating takes place, while membranes and aerogels conduct comparatively less interfacial heating
Salt-resistivity and anti-fouling behavior	Membranes can foul and aerogels can trap salts resulting in salt clogging	Designable (hydrophilic channels and salt-rejection strategies)	Many hydrogels succeed in preventing salt crystallization and have self-cleaning or anti-biofouling ability.
Contaminant removal	Usually, passive separation and requires added adsorbents or post-treatment	Intrinsic adsorption sites; tunable chemistry for dyes, metals and organics	Hydrogels possess multifunctionality, performing desalination, heavy metal/VOC removal, anti-bacterial activity, electricity generation and resource recovery.
Cost and scalability	Moderate (in terms of membranes) and high (in terms of aerogels)	Low/moderate; facilitating scalable fabrication	Hydrogels are scalable, having preparation simplicity using low-cost, low-energy-consuming methods, whereas membranes/aerogels have manufacturing complexities due to freeze-casting, advanced coating or high-cost supercritical drying processes.
Mechanical stability	Membranes are robust but less adaptive. Aerogels are fragile and brittle.	Flexible and easy to integrate with photothermal fillers (*e.g.* CDs)	Hydrogels can conform to irregular surfaces whereas membranes cannot withstand varying conditions and aerogels lack flexibility due to weak strain of covalent bonds and internal capillary pressure while drying.
Solar absorptivity	Restricted absorption, based on the design and materials used.	Can be tuned to improvise absorption of solar energy and heat conversion	Most hydrogels have broadband solar absorptivity (UV-vis-NIR region) whereas membranes and aerogels have lesser solar-to-thermal conversion efficiency, limiting vaporization rate.

an evaporation rate of 1.4 kg m^{-2} h^{-1} and a solar-driven evaporation efficacy of 89%. The SEM images depict the fibrous structure of the bare C-dot hydrogel {Fig. 14a(i) and (ii)}. Based on the practical applications of the C-dot/hydrogel composite for water purification, the recovery of purified water was measured following illumination in a solar stimulator (1 kW m^{-2} intensity) for 60 min. It can be seen that the calculated water recovery was less than 15% for the bare hydrogel while the percentage reached 55% for 20%-C-dot/hydrogel, as shown in (Fig. 14b). For the water remediation applications, particularly the removal of heavy metal ions, the decontamination efficiency was determined for Cu^{2+}, Ni^{2+}, Ag^{+}, and Cd^{2+}. The residual level of dissolved metal ion contaminants in aqueous phase encapsulated within a C-dot-20/gel before irradiation at 1 kW m^{-2} for 1 h was 0.01 M, which appreciably did not exceed 0.05% of the initial ionic content detected in the treated water (Fig. 14c). For examining solar-mediated water heating, the temperature of the C-dot/hydrogel was measured using an infrared (IR) camera, which demonstrated the impact of the C-dots on heating. It can be seen that after 60 min of illumination, the water-saturated 20% (w/w) C-dot/hydrogel attained a temperature of 58 °C, whereas the bare hydrogel reached a much lower temperature of 28 °C (Fig. 14d).

With progressing research, it remains a task to develop a newer material, which simultaneously exhibits flexibility, durability, cost-effectiveness and the ease of synthesis along with sufficient photothermal conversion and good overall performance. With this approach, Li *et al.*[151] reported cellulose hydrogels modified with sulfhydryl-based carbon dots (CDs-SH) showing remarkable specificity and susceptibility for heavy metals like Hg(II) along with solar vapor generation. The hydrogel displayed more than 98% adsorption efficiency with an extraction ability of 662.25 mg g^{-1}, the interesting part being the upcycling of the depleted absorbents through *in situ* sulfurization for solar steam generation. It exhibited a boosted evaporation rate of 1.30 kg m^{-2} h^{-1} with an efficacy of 88.3% at 1 kW m^{-2} solar illumination. This work presented a streamlined approach to repurpose exhausted materials into functional, value-added products through a sustainable route.

5.2. Recent advancements in carbon dot–hydrogel composites

The selection of materials that simultaneously provide flexibility, durability, ease of synthesis and cost-effectiveness is an essential factor. Taking this into account, Indriyati *et al.*[152] designed a hydrogel film based on poly(vinyl alcohol) incorporated with carbon dots (CDs) (Fig. 15a) having a breaking stress

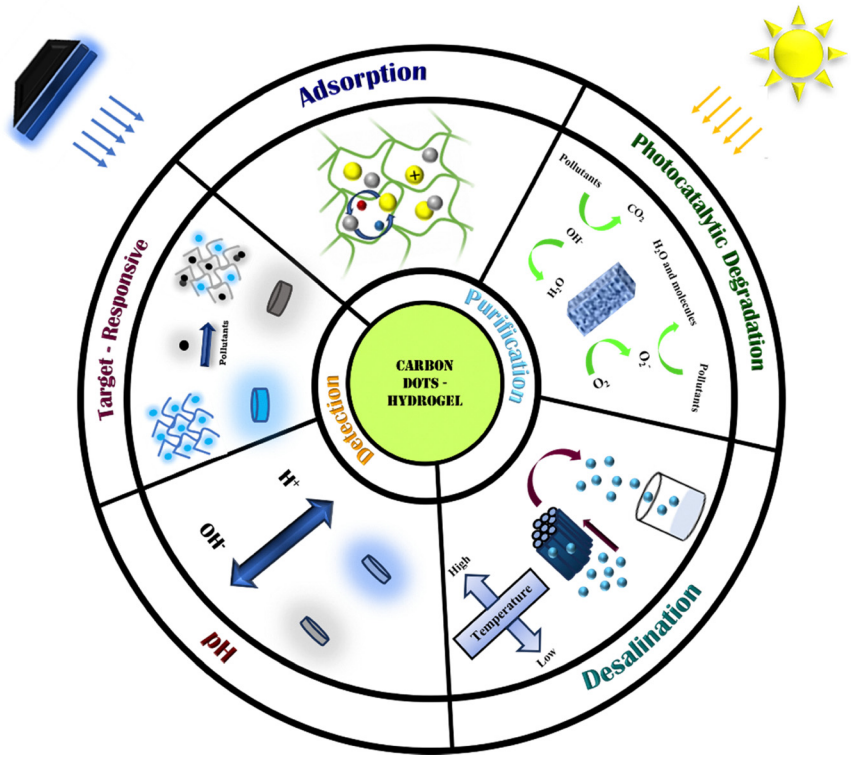

Fig. 13 Schematic of the overview of multifunctional CD–hydrogel systems: adsorption, photocatalysis, desalination, purification, sensing and target-responsive applications.

of 9 MPa and an elongation of 247%. Notably, the hydrophilic behaviour of PVA facilitated the improved water transport to the evaporation surface, resulting in an elevated rate of evaporation, *i.e.* 1.58 kg m^{-2} h^{-1} under one sun irradiation, which was found to be 6.1 times more than pure water excluding hydrogel (0.26 kg m^{-2} h^{-1}), also maintaining steady

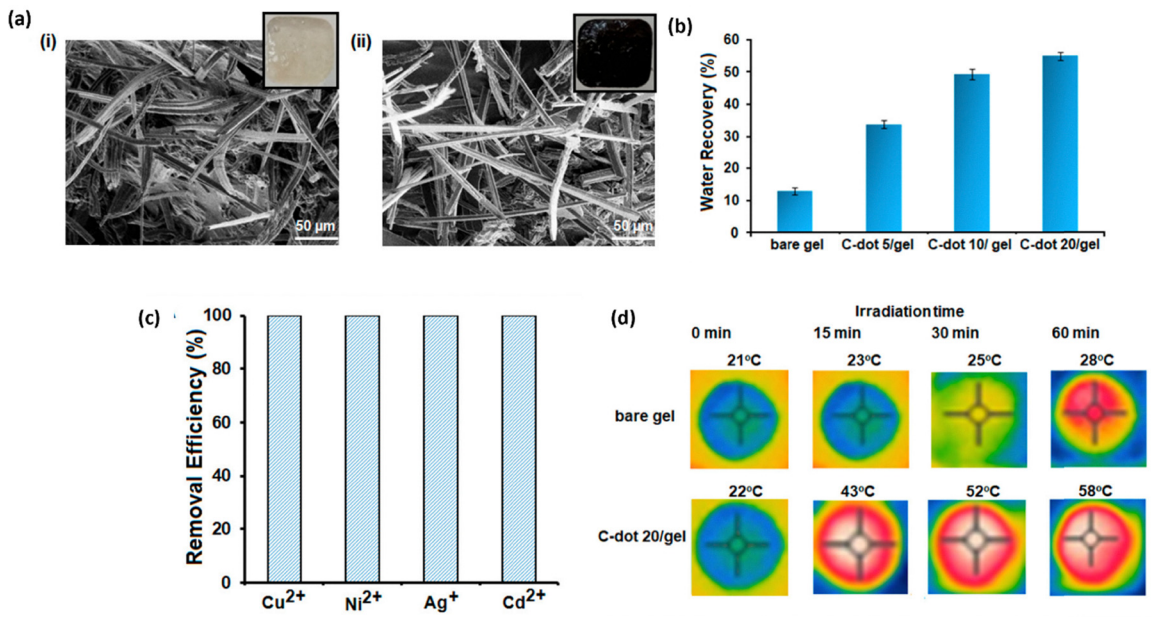

Fig. 14 (a) SEM images of (i) bare hydrogel and (ii) C-dot hydrogel with the photographs on the top right depicting the appearance of the gels. (b) Water recovery percentage in various C-dot hydrogels with solar illumination for 1 h. (c) Water purification applications showing the heavy metal ion removal efficiency. (d) Infrared images of the bare hydrogel and 20% C-dot hydrogel. Reprinted with permission from ref. 150. Copyright 2019 the American Chemical Society.

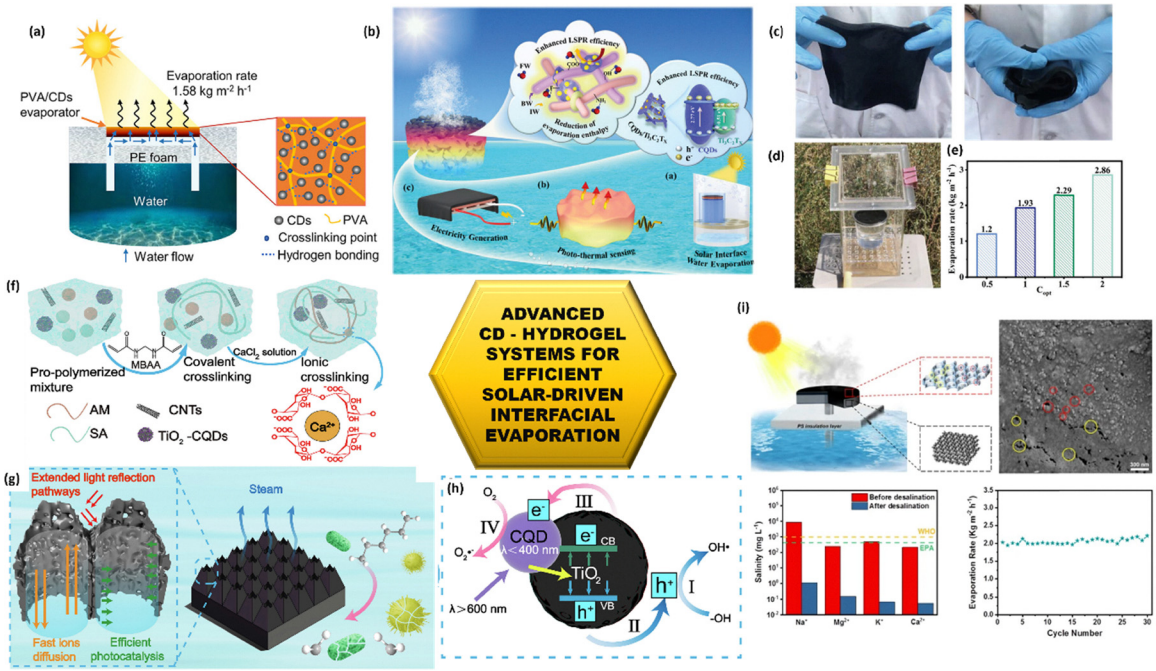

Fig. 15 Advanced CD–hydrogel systems for efficient solar-driven interfacial evaporation (a) schematic of the PVA/CD evaporator. Reprinted with permission from ref. 152. Copyright 2024 American Chemical Society. (b) Graphical representation of the enhanced LSPR effect in 0D CQDs/2D MXene/CMC/PAM hydrogel (c) large-sized evaporator and its folding ability. (d) Integrated device incorporating the hydrogel for outdoor experiments (e) evaporation rates at 0.5, 1, 1.5 and 2 suns, respectively. Reprinted with permission from ref. 153. Copyright 2024 Wiley-VCH GmbH. (f) Cross-linking mechanisms of the PSTCC evaporator. (g) Illustration of the evaporator's surface convex protrusions and vertical capillary pathways. (h) Charge-transfer mechanisms in CQDs–TiO_2 composite showing wavelength-dependent electron–hole migration (I and II) and formation of superoxide and hydroxyl radicals (III and IV). Reprinted with permission from ref. 154. Copyright 2025 Elsevier B.V. (i) Graphical representation of the bilayer structural carbon-based hydrogel depicting the morphological features, desalination performance and evaporation rates. Reprinted with permission from ref. 155. Copyright 2023 Science China Press.

evaporation rates over repeated cycles. Hybrid photothermal materials can be revolutionary to magnify the solar absorption, light-to-heat conversion capacity and design multipurpose solar evaporators. Herein, Jing *et al.*[153] combined 0D carbon quantum dots (CQDs) with 2D MXenes to act as the hybrid photothermal agents. Sodium carboxymethyl cellulose (CMC)/polyacrylamide (PAM) hydrogel was used as a substrate material to transport water for the reduction of evaporation enthalpy. The synergism between the carbon quantum dots and 2D MXene fastened the carrier transfer leading to localized surface plasmon resonance (LSPR) effect (Fig. 15b). The evaporator's large-size preparation (18 × 18 cm) exhibited remarkable folding ability, allowing transportation during scale-up applications (Fig. 15c). Outdoor experiments (Fig. 15d) showed higher evaporation rates of 1.93 and 2.86 kg m^{-2} h^{-1} under one and two sun irradiations, respectively (Fig. 15e), along with a lower evaporation enthalpy (1485 J g^{-1}). On applying for photothermal sensing and temperature difference power generation (TEG), the device presented a remarkable output power density of 230.7 mW m^{-2}. Advancement in the design and synthesis of bifunctional (photothermal and photocatalytic) materials broadens the scope of multi-purpose, versatile applications. Focusing on this, Liu *et al.*[154] presented the development of a bifunctional hydrogel device incorporating polyacrylamide, sodium alginate, titanium dioxide, carbon quantum dots and carbon nanotubes (PSTCC) (Fig. 15f). This evaporator was constructed with surface convex protrusions and vertically oriented capillary pathways (Fig. 15g), achieving an appreciable evaporation rate of 2.56 kg m^{-2} h^{-1} at 1 kW m^{-2} solar irradiation and photocatalytic degradation efficacy of 85.5% in case of methylene blue, thereby inactivating *Chlorella vulgaris* at a rate of 58.7% and eliminating organic contaminants. This incorporation prominently improvised the light-to-thermal conversion rate while efficiently tuning the bandgap of TiO_2 which elevated the photocatalytic behaviour (Fig. 15h). Along with other factors, scalability and portability are also major considerations. In this regard, Sun *et al.*[155] prepared a bilayer structural carbon-based hydrogel composite material obtaining an excellent rate of evaporation, *i.e.* 2.19 kg m^{-2} h^{-1} with an energy conversion efficacy of 93.7% at an irradiation of 1 kW m^{-2} over 30 repeated cycles. The composite exhibited a surged desalination performance (Fig. 15i) along with adaptability, scalability and flexibility, thus widening the horizon of its practical applications. Moreover, its cost-effectiveness and enhanced structural design make its implementation easy even in economically backward areas, exhibiting further advances as compared to the previously reported evaporators.

The presence of phenolic VOCs in the natural aquatic environment poses a serious threat as they evaporate more rapidly than water molecules during solar vapor generation.

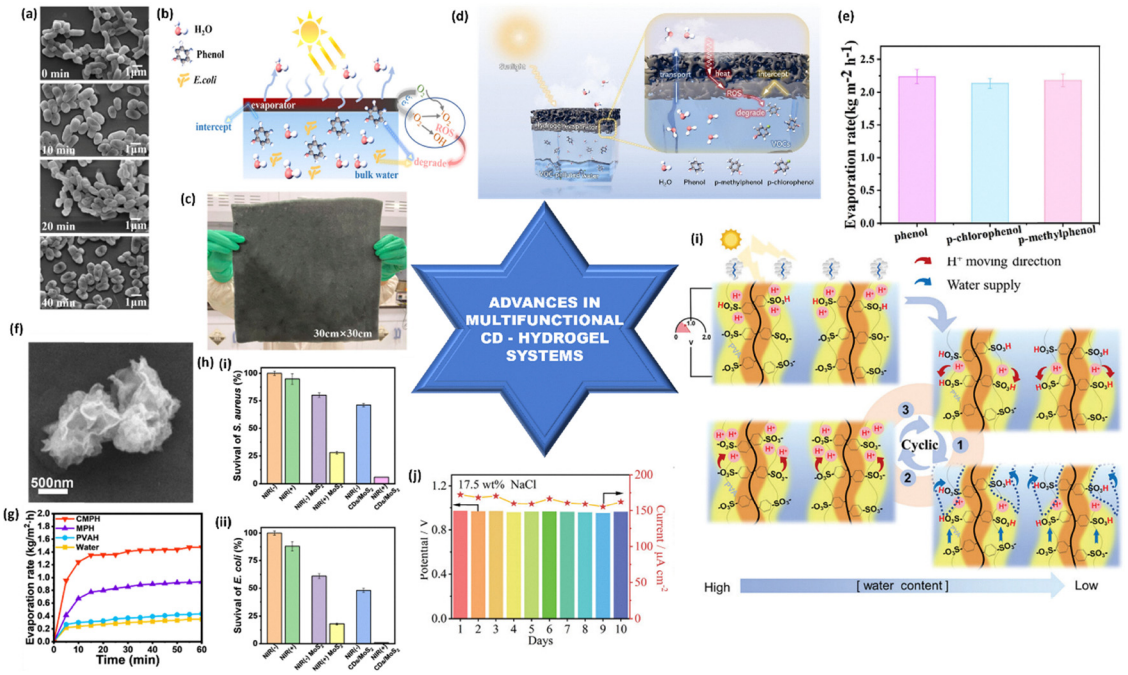

Fig. 16 (a) SEM images showing the inactivation of *E. coli* using the SA/CCC/Cu^{2+} hydrogel within 40 min. (b) Scheme representing the solar vaporization and VOC degradation. (c) Scalable synthesis of the hydrogel. Reprinted with permission from ref. 156. Copyright 2024 the American Chemical Society. (d) Illustration of the synergistic applications of CSE. (e) Evaporation rates during *p*-chlorophenol and *p*-methylphenol removal. Reprinted with permission from ref. 157. Copyright 2023 Elsevier B.V. (f) SEM micrograph of CDs/MoS_2. (g) Evaporation rates of CMPH achieved within 60 min. (h) Antibacterial activity of CMPH towards (i) *E. coli* and (ii) *S. aureus*. Reprinted with permission from ref. 158. Copyright 2024 Elsevier B.V. (i) Schematic of the evaporation-based consistent electric generation in GMS@HCDs. (j) Stability of electricity generation performance in 17.5 wt% NaCl. Reprinted with permission from ref. 159. Copyright 2024 Wiley-VCH GmbH.

Therein, the development of advanced materials is necessary which can synchronously carry out photothermal desalination along with the degradation of the VOCs. With this approach, An *et al.*[156] reported employing a Cu^{2+}-crosslinked sodium alginate (SA) hydrogel as the structural matrix with internally embedded carbonized carboxymethyl chitosan (CMC) as the photothermal agent, thereby integrating both photothermal and photocatalytic functionalities. This SA/CCC/Cu^{2+} hydrogel attained evident separation of distilled water from VOC-contaminated water, terminating VOCs with an efficiency of 96.74% alongside a notable evaporation rate of 2.54 kg m^{-2} h^{-1}. It further exhibited a potent antibacterial performance inactivating *E. coli* within 40 min completely as well as scalable production (Fig. 16a–c).

In order to eliminate VOCs with super adsorption-photocatalysis capability, the magical result of evaporation–adsorption–degradation has to be realized (Fig. 16d). Herein, An *et al.*[157] reported a carbonized CMC/SA solar evaporator (CSE) fabricated with the aim of synergistic desalination and VOC removal. The results reveal 95.37% removal efficiency of phenol and an evaporation rate of 2.24 kg m^{-2} h^{-1} (Fig. 16e). Moreover, this simple and affordable evaporator simultaneously removes different VOCs such as *p*-chlorophenol and *p*-methylphenol during the process of solar vapor generation.

With further advances, Li *et al.*[158] reported a work where a multi-defective MoS_2 nanoflower was hydrothermally synthesized in a carbon-dot medium to form CDs/MoS_2 (Fig. 16f) exhibiting a boost in the photothermal and catalytic performance due to structural and morphological modifications. An asymmetric (CDs/MoS_2@PVA) hydrogel evaporator (CMPH) fabricated *via* repeated freeze–thaw cycles facilitated gradient photothermal distribution, reduced channel blockage, improvised light trapping and hotspot formation with an evaporation rate of 1.49 kg m^{-2} h^{-1} and an efficiency of 92.5% under one sun illumination (Fig. 16g). The system also demonstrated multifunctional water treatment including 94% and 99% antibacterial activity against *S. aureus* and *E. coli*, respectively {Fig. 16h(i) and (ii)}, a remarkable decrease in the concentrations of four major ions (Na^+, Mg^{2+}, K^+ and Ca^{2+}) and 91% photodegradation of methylene blue, resulting in effective desalination and removal of organic compounds.

Interfacial evaporation materials absorb and convert solar energy while an adjacent collector transfers the absorbed heat into a thermoelectric converter, which transduces the thermal gradient into electrical power for storage or external utilization. Based on this, Li *et al.*[159] designed a solar-interfacial evaporation (SIE) power generation device (GMS@HCDs) by functionalizing a commercial melamine sponge with CD-coupled graphene and polyelectrolyte hydrogels assisting sustained electricity output driven by an evaporation-maintained proton concentration gradient (Fig. 16i). IW having reduced evaporation enthalpy evaporates from the interface driving the protons from polystyrene sulfonic acid groups to the bottom leading to

Table 4 Comparative study of the preparation methods, evaporation rate, stability, and salt resistance of various CD–hydrogel systems

System	Preparation method	Evaporation rate (kg m^{-2} h^{-1})	Stability (cycles/durability)	Salt resistivity
PVA/CD hydrogel film[152]	Mixing + solution casting (citric acid)	~1.58 (1 sun)	High (steady over repeated cycles)	Excellent (desalination)
3D CD/hydrogel sponge[149]	Encapsulation in porous hydrogel	~1.40 (1 sun)	High (offers recyclability)	Potent (heavy metal/salt elimination)
C-CDSA (carbonized CD–starch)[160]	Carbonization (270 °C)	2.29 (1 sun)	High (acid/alkali/organic stability)	High (10% NaCl)
PVA/GA/AC composite[161]	*In situ* polymerization	2.49 (1 sun)	High (consistent operability)	High (desalination/seawater)
CDs-PDA-SA[162]	C0-hydrothermal carbonization + polymerization of dopamine and SA	2.15 (3.92 with condenser)	Very high (waste-based)	Suitable for wastewater purification
PVA/CD-SP hydrogel[163]	Physical crosslinking/crystallization)	Highly efficient	Remarkable stability (more than 1100 cycles)	Possess stability (underwater sensing/seawater)
Lignin–CD/PVA film[164]	Blending + casting	Enhanced (photothermal)	Excellent (thermally stable)	High (blocking efficacy)
CDs-SCH (CMC/SA/AM)[165]	Free radical polymerization	Efficient	High (pH responsive/adsorption)	High (ion detection/adsorption)
Chitosan/carbon sponge-like hydrogel (CCH)[166]	Freeze-casting + alkali infiltration	4.23 (1.0 sun)/11.04 (4 sun)	Excellent (no salt-blockage in 15% brine	5-day consistent operability without cleaning

reverse dissociation. The cyclic process where FW fills the vaporized IW area results in proton dissociation and diffusion, FW replenishment and production of continuous current and voltage (Table 4). This device achieves an evaporation rate of 3.53 kg m^{-2} h^{-1} and consistent outputs of 0.972 V and 172.38 A cm^{-2} on operating in highly concentrated brine (17.5 wt% NaCl) (Fig. 16j).

5.3. Progress in device integration and scale-up applications

The device-level integration and mass production of CD–hydrogel-based solar evaporators mark a transformative progress in the field of sustainable water purification. Such integration facilitates real-world evaporator units to operate under natural sunlight producing cleaner water in resource-limited areas. It further validates the robustness of the hydrogel designs under varied environmental conditions, assessing durability and consistent operating stability. However, laboratory experimentations have already demonstrated ultra-high evaporation rates, salt elimination, and mechanical stability, as already discussed in the previous sections. Therefore, scaling these systems into deployable devices would bridge the gap between experimental innovation and societal impact, positioning them as a cornerstone solution for addressing global water scarcity.

In this view, Zhang *et al.*[167] demonstrated a prominent translation from laboratory innovation to practical application by homogeneously embedding CDs into a low-cost SA/PVA dual-crosslinked hydrogel backbone immobilized on a melamine sponge (MS), giving rise to 3D water transport channels. This scalable 3D-CDs/SA/PVA-MS hydrogel (Fig. 17a) showed a superior solar steam generation rate of 4.79 kg m^{-2} h^{-1} in a 3.5 wt% NaCl solution at 1 sun illumination and a comparatively remarkable evaporation rate of 4.13 kg m^{-2} h^{-1} in extremely saline seawater (25 wt%) (Fig. 17b). Outdoor experiments were carried out using a simple device assembly comprising the hydrogel material, compact condenser and storage units (Fig. 17c). The evaporation device was kept on the rooftop, noting the solar radiation intensity. It showed a notable evaporation efficiency with a huge amount of condensate appearing on the condenser within 30 min (Fig. 17d). The rate of evaporation elevated to 2.8 kg m^{-2} h^{-1} within 5 h of irradiation with the solar intensity peaking at 0.82 kW m^{-2} (Fig. 17e), thereby producing a consistent water yield of 14.2 kg m^{-2} over repeated cycles. Moreover, simulated organic dye and acidic and alkaline solutions were tested to assess the evaporator's water purification capacity. ICP measurements revealed the reduction of ion concentrations and the absence of organic dyes, particularly sodium (12.6 mg L^{-1}) reaching the standards set by the WHO.

With further advancements, Mate *et al.*[168] presented the successful development of a portable solar evaporator (F-CD-p@BC) by integrating a covalently bonded CD porphyrin network that accelerates broad light absorptivity into a bacterial cellulose hydrogel through the Alder–Longo reaction promoting multifunctional water treatment *i.e.* desalination, dye and heavy-metal removal, consistent solar evaporation and self-cleaning (Fig. 18a). Outdoor experiments were conducted by constructing a device constituting of an evaporation chamber where the hydrogel evaporator was mounted. This device was kept on the rooftop where subsequent condensation was observed within 1 hour and the water droplets were collected in a condenser (Fig. 18b). The evaporation rate was found to be 2.7 kg m^{-2} h^{-1} (Fig. 18c). Durability was also tested which revealed no evident decline in the evaporation rate after 10 cycles (Fig. 18d). It was also revealed that approximately 99% dyes were eliminated and the concentrations of Na^+, Mg^{2+}, Ca^{2+} and K^+ were evidently reduced below the limits set by the WHO (Fig. 18e). This F-CD-p@BC membrane exemplifies interfacial solar vapor generation from materials development to highly scalable, device-level progress.

6. Challenges and future directions

Solar-driven steam generation is a fast-growing technology for producing accessible and cleaner water, showing potential to

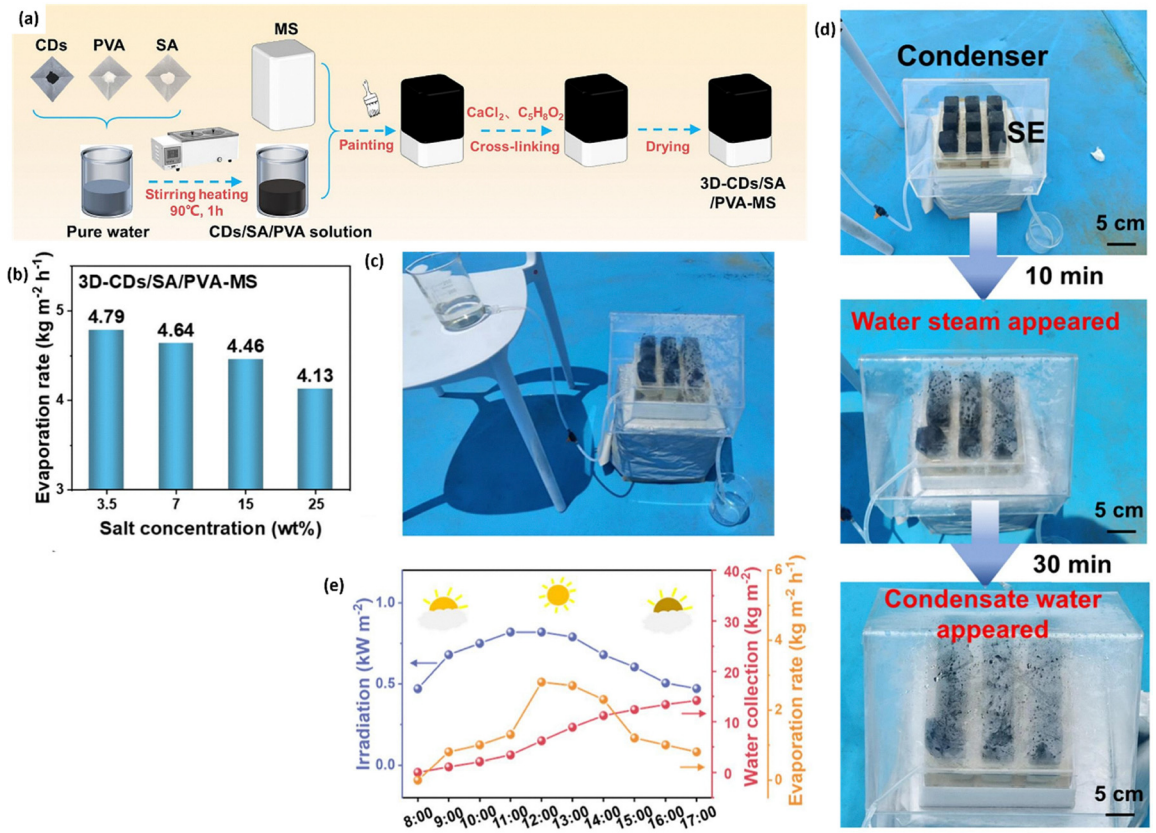

Fig. 17 (a) Model images of the 3D-CDs/SA/PVA-MS hydrogel. (b) Evaporation rates at different salt concentrations. (c) Digital image of the integrated evaporator desalination system. (d) Photographs showing the rapid steam generation within 30 min of irradiation. (e) Actual rate of evaporation during the outdoor experiment. Reprinted with permission from ref. 167. Copyright 2024 Elsevier B.V.

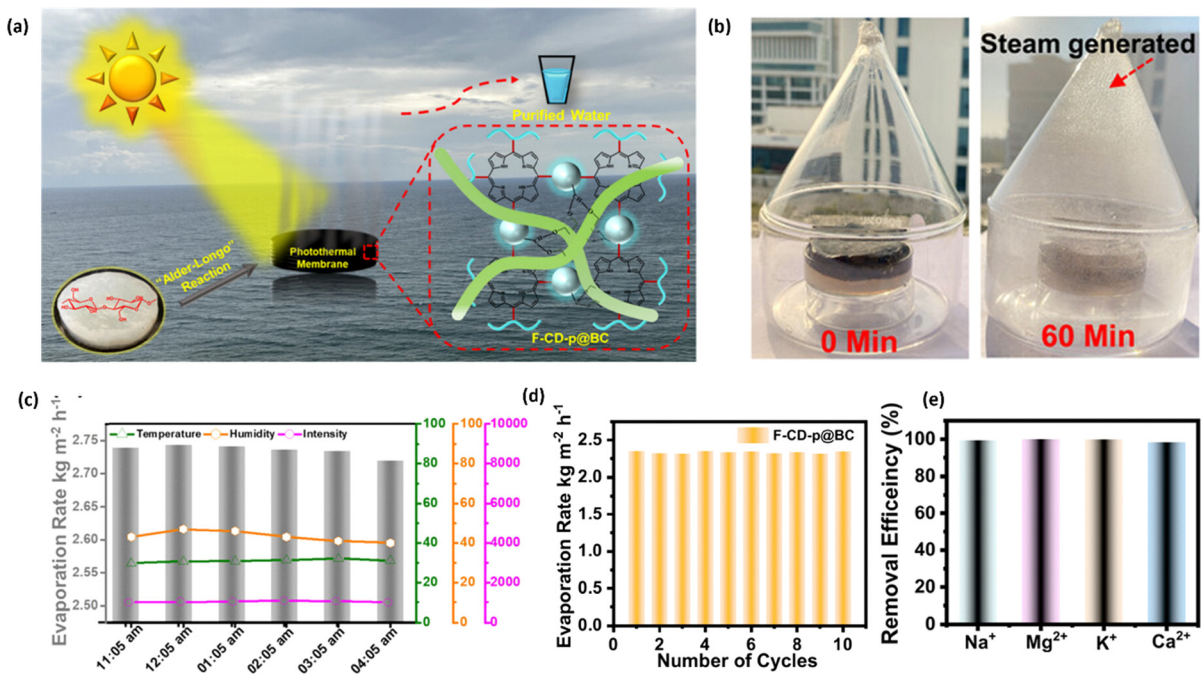

Fig. 18 (a) Schematic depicting the solar-driven evaporation using F-CD-p@BC. (b) Images showing the lab-made integrated device incorporating the evaporator generating steam at 0 and 60 min. (c) Freshwater rate of evaporation based on the outdoor test. (d) Evaporation rates recorded over 10 cycles. (e) Removal of ions from simulated seawater. Reprinted with permission from ref. 168. Copyright 2025 the American Chemical Society.

successfully meet the escalating global need for the availability of freshwater, ecological preservation and sustainable energy solutions. This paper reviews the enormous progression of hydrogel-engineered solar water treatment systems. Moreover, despite the currently achieved goals, a massive part of the research and design have become stagnant in the laboratory stage; therefore, there remains challenges to tackle along with large-scale production and industrialisation. The salient challenges for future solar evaporation research and practical applications are listed here:

(1) Fundamental and theoretical limitations: a mechanistic understanding of polymer–water, polymer–solute and polymer–CD interactions, specifically at the complex and molecular scale is required. The underdeveloped rational design of hydrogel building blocks and advanced *in situ* characterization techniques demand more scientific focus to elucidate evaporation dynamics at the hydrogel–air interface.

(2) Control of water states and energy efficiency: optimization of BW, FW and IW states is crucial for further reducing the evaporation enthalpy. Introducing hierarchical nanostructured pore engineering is needed to boost the IW content. Moreover, achieving a balance between water transport and evaporation rate remains a critical design constraint.

(3) Material stability and durability: long-term performance is hindered by photochemical degradation (UV-induced oxidation and polymer chain scission) and mechanical stress from wet-dry cycling and varying environmental conditions. Therefore, chemically and physically robust designs such as multi-network hydrogels are needed to enhance the mechanical strength, photostability and structural integrity.

(4) Fouling, contamination and chemical resistance: biofouling, organic pollutants and salt crystallization clog transport channels. Highly saline and multivalent ions disrupt polymer networks through salting-out effects and coordination interactions. Future designs must incorporate antibiofouling and self-cleaning functionalities, salt resistant and ion-tolerant polymer networks, surface engineering and protective coatings.

(5) Incomplete removal of volatile contaminants: volatile organic compounds (VOCs) co-evaporate with water, limiting the purification efficiency. Further intensive research on integrating photocatalytic or multifunctional materials and developing multibarrier purification systems will be beneficial for their complete degradation.

(6) Light utilization and environmental adaptability: environmental conditions like variable solar intensity, temperature and humidity significantly affect the overall efficacy. Current evaporation systems lack adaptive light-harvesting capabilities. They should incorporate omnidirectional or self-tracking light absorption for potent operation under low-light, non-ideal and nocturnal conditions.

(7) Water collection: the overall system efficacy relies not only on evaporation but also on condensation efficiency, collection and storage of purified water. Preventing secondary contamination, elevating vapor condensation rates and universally adopted standardized protocols for evaluating water evaporation rate (WER) and photothermal conversion efficiency (PCE) still needs to be addressed.

(8) Scalability, cost and design constraints: large-scale deployment is limited by complex fabrication techniques and high material and processing costs. Focus should be on low-cost, abundant and environmentally benign materials, scalable fabrication methods (*e.g.* 3D printing) and simple but high-throughput manufacturing processes.

(9) Environmental sustainability and multifunctionality: this opts for eco-friendly synthesis routes and reduced material waste or emissions. Life-cycle assessment is necessary to evaluate the environmental impact and biocompatibility. Developing further evolved hydrogel evaporators with multifunctional platforms for salt/metal recovery (zero liquid discharge), wastewater treatment, atmospheric water harvesting and simultaneous electricity generation (*via* thermal, salinity or evaporation gradients) is necessary.

(10) Resource recovery and practical deployment: localized salt crystallization facilitates controlled salt-accumulation through guided internal water transport, allowing salt to crystallize in specific peripheral areas (edges) and recovering the solid salt. A distinct gap also persists between laboratory-scale performance and real-world implementation, which needs to be filled with the development of portable, flexible and large-scale systems for community-level desalination under diverse water sources.

7. Conclusion and outlook

CD-integrated hydrogel solar vapor generation systems have emerged as transformative and potent next-generation platforms for sustainable water purification offering a synergistic integration of efficient CDs within structurally tunable hydrogel networks, enabling long-term solar-to-thermal conversion, water transport regulation and heat localization. This review outlined the unique physiochemical properties of hydrogels, notably their porous architecture, adjustable wettability and water states modulation that play a decisive role in enhancing the evaporation kinetics while minimizing the energy consumption. Moreover, innovations in surface topography, multifunctional material incorporation and structural optimization collectively lead to superior evaporation performance and operational versatility. Despite these achievements, the field remains in a developmental phase with critical challenges that impede the transition from laboratory-scale to real-world applications. Concurrently, factors such as prolonged photochemical and mechanical stability, fouling resistance, salt accumulation and incomplete removal of VOCs remain the key bottlenecks. Moreover, practical deployment and commercialization is constrained by scalability, cost-effectiveness, environmental adaptability and the need for efficient vapor condensation and collection strategies. Future progress in this domain demands a paradigm shift towards a holistic and interdisciplinary approach focusing on integrated systems that optimally balance remarkable performance with durability,

economic viability and sustainability. Identifying multifunctionalities (*e.g.* antibiofouling, photocatalysis and energy co-generation) and optimizing light-harvesting designs and resource recovery will be pivotal. Equally important is the need for standardized testing protocols and persistent field validation to ensure reliability. Continued innovation surrounding materials science, structural engineering and system integration can pave the way to address the global water-energy nexus evolving from laboratory-scale prototypes to scalable, real-world solutions.

Conflicts of interest

There are no conflicts to declare.

Data availability

No primary research results, software or codes have been included, and no new data were generated or analysed as part of this review.

References

1 P. Verma, B. Sharma, S. Dhar, P. Mehta and A. K. Taloor, A survey on water resource availability for sustainable water management practices in the UT of J&K, *Discover Geosci.*, 2025, **3**, 110.
2 A. Boretti and L. Rosa, Reassessing the projections of the World Water Development Report, *npj Clean Water*, 2019, **2**, 15.
3 A. K. Pandey, Sustainable water management through integrated technologies and circular resource recovery, *Environ. Sci.: Water Res. Technol.*, 2025, **11**, 1822–1846.
4 M. Wang, B. L. Bodirsky, R. Rijneveld, F. Beier, M. P. Bak, M. Batool, B. Droppers, A. Popp, M. T. H. V. Vliet and M. Strokal, A triple increase in global river basins with water scarcity due to future pollution, *Nat. Commun.*, 2024, **15**, 880.
5 K. Javan, A. Altaee, S. BaniHashemi, M. Darestani, J. Zhou and G. Pignatta, A review of interconnected challenges in the water–energy–food nexus: Urban pollution perspective towards sustainable development, *Sci. Total Environ.*, 2024, **912**, 169319.
6 J. Liu, R. Li and B. Yang, Carbon Dots: A New Type of Carbon-Based Nanomaterial with Wide Applications, *ACS Cent. Sci.*, 2020, **6**, 2179–2195.
7 B. Wang, H. Cai, G. I. N. Waterhouse, X. Qu, B. Yang and S. Lu, Carbon Dots in Bioimaging, Biosensing and Therapeutics: A Comprehensive Review, *Small Sci.*, 2022, **2**, 2200012.
8 S. Goyal, S. Chaudhary, A. Umar and A. A. Ibrahim, Carbon Dots in Catalysis: Synthesis, Properties, Applications, Comparative Advantages, and Future Directions, *J. Environ. Chem. Eng.*, 2025, **13**, 115556.
9 E. A. Stepanidenko, E. V. Ushakova, A. V. Fedorov and A. L. Rogach, Applications of Carbon Dots in Optoelectronics, *Nanomaterials*, 2021, **11**, 364.
10 K. Barrientos, J. P. Arango, M. S. Moncada, J. Placido, J. Patino, S. L. Macias, C. Maldonado, S. Torijano, S. Bustamante, M. E. Londono and M. Jaramillo, Carbon dot-based biosensors for the detection of communicable and non -communicable diseases, *Talanta*, 2023, **251**, 123791.
11 S. Singh, N. Shauloff and R. Jelinek, Solar-Enabled Water Remediation *via* Recyclable Carbon Dot/Hydrogel Composites, *ACS Sustainable Chem. Eng.*, 2019, **7**, 13186–13194.
12 K. Ramzy, I. Elbatal, E. M. Almetwally, E. A. AbdelAziz and M. Bassyouni, Advances and challenges in sustainable solar desalination for freshwater production, *Sol. Energy*, 2026, **304**, 114190.
13 A. Selvam, G. Jain, R. G. Chaudhari, M. K. Mandal and S. Chakrabarti, Avant-Garde Solar–Thermal Nanostructures: Nascent Strategy into Effective Photothermal Desalination, *Sol. RRL*, 2022, **6**, 2200321.
14 X. Ren, X. Li, H. He, G. Chen, D. Li, J. Lv, Y. Zhang, J. Yu, Y. Guan, Y. Qu, R. Xu and Y. Wu, Solar-driven interfacial evaporation technologies: Materials, optimization strategies, applications, and research progress, *eScience Energy*, 2026, **2**, 100028.
15 L. Hou, S. Li, Y. Qi, J. Liu, Z. Cui, X. Liu, Y. Zhang, N. Wang and Y. Zhao, Advancing Efficiency in Solar-Driven Interfacial Evaporation: Strategies and Applications, *ACS Nano*, 2025, **19**, 9636–9683.
16 P. Cheng, D. Wang and P. Schaaf, A Review on Photothermal Conversion of Solar Energy with Nanomaterials and Nanostructures: From Fundamentals to Applications, *Adv. Sustainable Syst.*, 2022, **6**, 2200115.
17 J. Zhu, L. Huang, F. Bao, G. Chen, K. Song, Z. Wang, H. Xia, J. Gao, Y. Song, C. Zhu, F. Lu, T. Zheng and M. Ji, Carbon materials for enhanced photothermal conversion: Preparation and applications on steam generation, *Mater. Rep.: Energy*, 2024, **4**, 100245.
18 N. Hasan, G. A. K. M. R. Bari and J. H. Jeong, Emerging Material Design Trends in Photothermal Water Vapor Generation, *Int. J. Energy Res.*, 2025, **2025**, 9016908.
19 Y. Li, Y. Shi, H. Wang, T. Liu, X. Zheng, S. Gao and J. Lu, Recent advances in carbon-based materials for solar-driven interfacial photothermal conversion water evaporation: Assemblies, structures, applications, and prospective, *Carbon Energy*, 2023, **5**, e331.
20 W. Guan, Y. Guo and G. Yu, Carbon Materials for Solar Water Evaporation and Desalination, *Small*, 2021, **17**, 2007176.
21 X. Xu, Q. Chang, C. Xue, N. Li, H. Wang, J. Yang and S. Hu, A carbonized carbon dot-modified starch aerogel for efficient solar-powered water evaporation, *J. Mater. Chem. A*, 2022, **10**, 11712–11720.
22 Y. Wang, C. Wang, X. Song, S. K. Megarajan and H. Jiang, A facile nanocomposite strategy to fabricate a rGO–MWCNT photothermal layer for efficient water evaporation, *J. Mater. Chem. A*, 2018, **6**, 963–971.

23 R. Yan, Z. Huang, Y. Chen, L. Zhang and X. Sheng, Phase change composite based on lignin carbon aerogel/nickel foam dual-network for multisource energy harvesting and superb EMI shielding, *Int. J. Biol. Macromol.*, 2024, **277**, 134233.
24 B. Hou, D. Kong, J. Qian, Y. Yu, Z. Cui, X. Liu, J. Wang, T. Mei, J. Li and X. Wang, Flexible and portable graphene on carbon cloth as a power generator for electricity generation, *Carbon*, 2018, **140**, 488.
25 Y. Zhang, H. Wang, X. Wang, B. Liu and Y. Wei, An anti-oil-fouling and robust superhydrophilic $MnCo_2O_4$ coated stainless steel mesh for ultrafast oil/water mixtures separation, *Sep. Purif. Technol.*, 2021, **264**, 118435.
26 M. Aizudin, R. Goei, A. J. Ong, Y. Z. Tan, S. K. Lua, R. P. Pottammel, H. Geng, X. L. Wu, A. L. Y. Tok and E. H. Ang, Sustainable development of graphitic carbon nanosheets from plastic wastes with efficient photothermal energy conversion for enhanced solar evaporation, *J. Mater. Chem. A*, 2022, **10**, 19612–19617.
27 M. A. Rafea, A. Eid and W. M. Daoush, Synthesis and characterization of carbon nanotube/copper oxide nanocomposite as an enhanced absorber for solar radiation, *Opt. Mater.*, 2023, **138**, 113643.
28 J. B. Cheng, H. G. Shi, M. Cao, T. Wang, H. B. Zhao and Y. Z. Wang, Porous carbon materials for microwave absorption, *Mater. Adv.*, 2020, **1**, 2631–2645.
29 P. Tao, G. Ni, C. Song, W. Shang, J. Wu, J. Zhu, G. Chen and T. Dang, Solar-driven interfacial evaporation, *Nat. Energy*, 2018, **3**, 1031–1041.
30 H. Ghasemi, G. Ni, A. M. Marconnet, J. Loomis, S. Yerci, N. Miljkovic and G. Chen, Solar steam generation by heat localization, *Nat. Commun.*, 2014, **5**, 4449.
31 Y. Li, G. Bai, S. Zeng and J. Hao, Theranostic Carbon Dots with Innovative NIR-II Emission for in Vivo Renal-Excreted Optical Imaging and Photothermal Therapy, *ACS Appl. Mater. Interfaces*, 2019, **11**, 4737–4744.
32 S. Balou, P. Shandilya and A. Priye, Carbon dots for photothermal applications, *Front. Chem.*, 2022, **10**, 1023602.
33 S. Parveen, G. Singh and S. Husain, Synthesis of Carbon Dots from Waste: An Efficient Approach for Sustainable Environment, *ACS Symp. Ser.*, 2025, **1494**(11), 249–278 eISBN: 9780841296619.
34 J. Li, L. Wang, G. Jiang, Y. Wan, J. Wang, Y. Li and F. Pi, Luminescent carbon dots-rooted polysaccharide cross-linked hydrogel adsorbent for sensitive determination and efficient removal of Cu^{2+}, *Food Chem.*, 2024, **447**, 138977.
35 B. Wang and S. Lu, The light of carbon dots: From mechanism to applications, *Matter*, 2022, **5**, 110–149.
36 M. Liu, Optical Properties of Carbon Dots: A Review, *Nanoarchitectonics*, 2020, **1**, 2.
37 P. P. Falara, A. Zourou and K. V. Kordatos, Recent advances in Carbon Dots/2-D hybrid materials, *Carbon*, 2022, **195**, 219–245.
38 X. Wei, X. Wang, Y. Fu, X. Zhang and F. Yan, Emerging trends in CDs@hydrogels composites: from materials to applications, *Microchim. Acta*, 2024, **191**, 355.
39 A. M. M. Hasan, M. A. Hasan, A. Reza, M. M. Islam and M. A. B. H. Susan, Carbon dots as nano-modules for energy conversion and storage, *Mater. Today Commun.*, 2021, **29**, 102732.
40 S. Gengan, H. C. A. Murthy, M. Sillanpaa and T. Nhat, Carbon dots and their application as photocatalyst in dye degradation studies- Mini review, *Results Chem.*, 2022, **4**, 100674.
41 N. A. A. Nazri, N. H. Azeman, Y. Luo and A. A. A. Bakar, Carbon quantum dots for optical sensor applications: A review, *Opt. Laser Technol.*, 2021, **139**, 106928.
42 L. P. Li, X. F. Ren, P. R. Bai, Y. Liu, W. Y. Xu, J. Xie and R. P. Zhang, Near-infrared emission carbon dots for bioimaging applications, *New Carbon Mater.*, 2021, **36**, 632–638.
43 W. Li, Y. Han, L. Wang, G. S. Selopal, X. Wang and H. Zhao, Highly bright solid-state carbon dots for efficient anticounterfeiting, *RSC Adv.*, 2024, **14**, 83–89.
44 W. Su, H. Wu, H. Xu, Y. Zhang, Y. Li, X. Li and L. Fan, Carbon dots: a booming material for biomedical applications, *Mater. Chem. Front.*, 2020, **4**, 821–836.
45 W. Pholauyphon, R. N. Bulakhe, J. Manyam, I. In and P. Paoprasert, High-performance supercapacitors using carbon dots/titanium dioxide composite electrodes and carbon dot-added sulfuric acid electrolyte, *J. Electroanal. Chem.*, 2022, **910**, 116177.
46 Y. Li and Y. Zou, Conjugated Polymer Photovoltaic Materials with Broad Absorption Band and High Charge Carrier Mobility, *Adv. Mater.*, 2008, **20**, 2952–2958.
47 Y. Shi, N. Meng, Y. Wang, Z. Cheng, W. Zhang and Y. Liao, Scalable fabrication of conjugated microporous polymer sponges for efficient solar steam generation, *ACS Appl. Mater. Interfaces*, 2022, **14**, 4522–4531.
48 S. H. Park, J. H. Park, J. Kim and S. J. Lee, Simultaneous solar-driven seawater desalination and spontaneous power generation using polyvalent crosslinked polypyrrole/alginate hydrogels, *Desalination*, 2020, **500**, 114900.
49 Y. Wu, L. Shen, C. Zhang, H. Gao, J. Chen, L. Jin, P. Lin, H. Zhang and Y. Xia, Polyacid doping-enabled efficient solar evaporation of polypyrrole hydrogel, *Desalination*, 2021, **505**, 114766.
50 X. Zhao, Y. Chen, Y. Yin, L. Zou, Q. Chen, K. Liu, P. Lin, H. Su and Y. Chen, Janus Polypyrrole Nanobelt@polyvinyl Alcohol Hydrogel Evaporator for Robust Solar- Thermal Seawater Desalination and Sewage Purification, *ACS Appl. Mater. Interfaces*, 2021, **13**, 46717–46726.
51 X. Yin, Y. Zhang, Q. Guo, X. Cai, J. Xiao, Z. Ding and J. Yang, Macroporous Double- Network Hydrogel for High-Efficiency Solar Steam Generation Under 1 sun Illumination, *ACS Appl. Mater. Interfaces*, 2018, **10**, 10998–11007.
52 F. Zhu, L. Wang, B. Demir, M. An, Z. L. Wu, J. Yin, R. Xiao, Q. Zheng and J. Qian, Accelerating solar desalination in brine through ion activated hierarchically porous polyion complex hydrogels, *Mater. Horiz.*, 2020, **7**, 3187–3195.

53 X. Xu, S. Ozden, N. Bizmark, C. B. Arnold, S. S. Datta and R. D. Priestley, A Bioinspired Elastic Hydrogel for Solar-Driven Water Purification, *Adv. Mater.*, 2021, **33**, 2007833.
54 M. Pi, X. Wang, Z. Wang and R. Ran, Sustainable MXene/PDA hydrogel with core shell structure tailored for highly efficient solar evaporation and long-term desalination, *Polymer*, 2021, **230**, 124075.
55 S. Chaule, J. Hwang, S. J. Ha, J. Kang, J. C. Yoo and J. H. Jang, Rational Design of a High Performance and Robust Solar Evaporator via 3D-Printing Technology, *Adv. Mater.*, 2021, **33**, 2102649.
56 X. Zhao, Y. Chen, Y. Yin, L. Zou, Q. Chen, K. Liu, P. Lin, H. Su and Y. Chen, Janus Polypyrrole Nanobelt@polyvinyl Alcohol Hydrogel Evaporator for Robust Solar- Thermal Seawater Desalination and Sewage Purification, *ACS Appl. Mater. Interfaces*, 2021, **13**, 46717–46726.
57 W. Alhejaili, K. Lotfy and A. El-Bary, Photo-elasto-thermodiffusion waves of semiconductor with ramp-type heating for electrons-holes-coupled model with initial stress, *Wave Random Complex Media*, 2022, **35**, 2115–2133.
58 M. Umlauff, J. Hoffmann, H. Kalt, W. Langbein, J. M. Hvam, M. Scholl, J. Sollner, M. Heuken, B. Jobst and D. Hommel, Direct observation of free-exciton thermalization in quantum-well structures, *Phys. Rev.*, 2022, **B57**, 1390–1393.
59 Y. Lu, D. Fan, Y. Wang, H. Xu, C. Lu and X. Yang, Surface Patterning of Two- Dimensional Nanostructure-Embedded Photothermal Hydrogels for High-Yield Solar Steam Generation, *ACS Nano*, 2021, **15**, 10366–10376.
60 Z. Sun, Z. Li, W. Li and F. Bian, Mesoporous cellulose/TiO2/SiO2/TiN-based nanocomposite hydrogels for efficient solar steam evaporation: low thermal conductivity and high light-heat conversion, *Cellulose*, 2020, **27**, 481–491.
61 X. Li, J. Huang, L. Guo, X. Jin, L. Wang, Y. Deng, H. Xie and L. Ye, Efficient solar seawater desalination constructed by oxide composite hydrogel with chitin as the base, *Inorg. Chem. Commun.*, 2021, **129**, 108651.
62 X. Ming, A. Guo, G. Wang and X. Wang, Two-dimensional defective tungsten oxide nanosheets as high performance photo-absorbers for efficient solar steam generation, *Sol. Energy Mater. Sol. Cells*, 2018, **185**, 333–341.
63 M. Cao, Z. Chang, J. Tan, X. Wang, P. Zhang, S. Lin, J. Liu and A. Li, Superoxide radical-mediated self-synthesized Au/MoO (3-x) hybrids with enhanced peroxidase like activity and photothermal effect for anti-MRSA therapy, *ACS Appl. Mater. Interfaces*, 2022, **14**, 13025–13037.
64 M. Pi, X. Wang, Z. Wang and R. Ran, Sustainable MXene/PDA hydrogel with core shell structure tailored for highly efficient solar evaporation and long-term desalination, *Polymer*, 2021, **230**, 124075.
65 Y. Guo, X. Zhou, F. Zhao, J. Bae, B. Rosenberger and G. Yu, Synergistic energy nanoconfinement and water activation in hydrogels for efficient solar water desalination, *ACS Nano*, 2019, **13**, 7913–7919.
66 C. Xiao, W. Liang, Q.-M. Hasi, L. Chen, J. He, F. Liu, C. Wang, H. Sun, Z. Zhu and A. Li, Ag/polypyrrole co-modified poly(ionicliquid)s hydrogels as efficient solar generators for desalination, *Mater. Today Energy*, 2020, **16**, 100417.
67 A. Abdullah, A. Joseph, W. H. Alawee, M. Elashmawy, M. E. H. Attia, S. W. Sharshir and A. El-Harairy, The role of copper oxide nanomaterials in solar desalination: a systematic review of integration strategies, *Mater. Adv.*, 2026, **7**, 4037–4060.
68 G. Divyapriya, A. Rahman, W. Leng, W. Wang and P. J. Vikesland, One-step biosynthesis of a bilayered graphene oxide embedded bacterial nanocellulose hydrogel for versatile photothermal membrane applications, *Environ. Sci.: Nano*, 2022, **9**, 1639–1650.
69 C. Tian, C. Li, D. Chen, Y. Li, L. Xing, X. Tian, Y. Cao, W. Huang, Z. Liu and Y. Shen, Sandwich hydrogel with confined plasmonic Cu/carbon cells for efficient solar water purification, *J. Mater. Chem. A*, 2021, **9**, 15462–15471.
70 Z. Wang, F. Meng, X. Liu, Z. Gong, Y. Li, T. Lu, Y. Yao, M. Xu and L. Pan, Cellulose aerogel evaporators with vertical channels inspired by lotus rods for highly efficient solar water evaporation, *Desalination*, 2024, **591**, 118048.
71 Z. Zhang, Q. Zhang, H. Zhang, X. Zuo, Q. Yang, H. Tang, S. Jin and G. Li, A 3D aerogel evaporator for efficient solar interfacial evaporation: Breaking through the upper limit of steam production rate, *Chem. Eng. J.*, 2024, **499**, 156520.
72 T. Zhang, X. Wang, Y. Zhao, Y. Sun, X. Liu, H. Xie, J. He, S. Cui and L. Luo, Facile hydrogel foam evaporator for long-term desalination treatment of seawater, *Environ. Chem. Eng.*, 2026, **14**, 122736.
73 C. Ji, T. Wang, Y. Wang and H. Yang, Highly efficient solar water evaporation by wood through one-step in-situ synthesis of carbon dots, *Chem. Eng. J.*, 2024, **479**, 147680.
74 D. Hu, Z. Zhang, G. Zhang, G. Zhang and C. Ma, Self-Generating Zwitterionic Polyurethane Foam for Solar-Driven Water Evaporation in Complex Environments, *ACS Appl. Mater. Interfaces*, 2025, **17**, 17346–17357.
75 Y. Guo, F. Zhao, X. Zhou, Z. Chen and G. Yu, Tailoring Nanoscale Surface Topography of Hydrogel for Efficient Solar Vapor Generation, *Nano Lett.*, 2019, **19**, 2530–2536.
76 Y. Guo and G. Yu, Engineering Hydrogels for Efficient Solar Desalination and Water Purification, *Acc. Mater. Res.*, 2021, **2**, 374–384.
77 Y. Guo, X. Zhao, F. Zhao, Z. Jiao, X. Zhou and G. Yu, Tailoring Surface Wetting States for Ultrafast Solar-Driven Water Evaporation, *Energy Environ. Sci.*, 2020, **13**, 2087–2095.
78 Y. Liu, S. Yu, R. Feng, A. Bernard, Y. Liu, Y. Zhang, H. Duan, W. Shang, P. Tao, C. Song and T. Deng, A bioinspired, reusable, paper-based system for high performance large-scale evaporation, *Adv. Mater.*, 2015, **27**, 2768–2774.
79 W. Xu, Y. Xing, J. Liu, H. Wu, Y. Cui, D. Li, D. Guo, C. Li, A. Liu and H. Bai, Efficient Water Transport and Solar Steam Generation *via* Radially, Hierarchically Structured Aerogels, *ACS Nano*, 2019, **13**, 7930–7938.

80 S. Yu, Y. Zhang, H. Duan, Y. Liu, X. Quan, P. Tao, W. Sahng, J. Wu, C. Song and T. Deng, The impact of surface chemistry on the performance of localized solar-driven evaporation system, *Sci. Rep.*, 2015, **5**, 13600.
81 J. Liu, W. Ruan, H. Zhang, J. Huang, J. Wang, J. Wang, J. Fu, F. Sun, L. Zhu, Y. Zhan and J. Ma, Highly Efficient Porous Glass Solar Water Evaporator, *Adv. Funct. Mater.*, 2025, **35**, 2415394.
82 Z. Gui and D. Xiang, Hierarchically designed evaporators with dual-layered hydrogel/aerogel structure for efficient solar water evaporation, *Sep. Purif. Technol.*, 2023, **310**, 123237.
83 V. M. Gun'ko, I. N. Savina and S. V. Mikhalovsky, Properties of Water Bound in Hydrogels, *Gels*, 2017, **3**, 37.
84 F. Zhao, X. Zhou, Y. Shi, X. Qian, M. Alexander, X. Zhao, S. Mendez, R. Yang, L. Qu and G. Yu, Highly Efficient Solar Vapour Generation Via Hierarchically Nanostructured Gels, *Nat. Nanotechnol.*, 2018, **13**, 489–495.
85 C. Huang, Z. Wang, X. Zhao, X. Bao, C. Guo, W. Hou and H. Song, Hydrogel-Based Solar-Driven Interfacial Evaporation and Seawater Desalination, *Adv. Mater. Technol.*, 2025, **10**, e01477.
86 T. Terada, Y. Maeda and H. Kitano, Raman Spectroscopic Study on Water in Polymer Gels, *J. Phys. Chem.*, 1993, **97**, 3619–3622.
87 X. Zhou, Y. Guo, F. Zhao, W. Shi and G. Yu, Topology Controlled Hydration of Polymer Network in Hydrogels for Solar Driven Wastewater Treatment, *Adv. Mater.*, 2020, **32**, 2007012.
88 X. Zhang, H. Na, D. Liu and H. Li, Hydrogel-Based Solar Interfacial Evaporators: Design, Performance, and Applications, *Processes*, 2025, **13**, 3921.
89 Z. Li, F. Liu, X. Jing, W. Zhou, S. Pei, T. Abdiryim, F. Xu, J. You, Y. Tan and X. Liu, Ti_3C_2Tx/CuO composite hydrogels with low evaporation enthalpy and efficient photothermal conversion for solar-driven water purification, electricity generation and pollutant degradation, *Chem. Eng. J.*, 2025, **519**, 165019.
90 W. He, G. Xu, L. Xiang, Y. Liu, X. Zhang, Y. Yin and C. N. Markides, A novel solar-driven interfacial evaporator with multi-stage tunable liquid supply for efficient adaptive evaporation inspired by human thermal sweating, *Chem. Eng. J.*, 2025, **509**, 161249.
91 H. T. Kim, L. Philip, A. McDonagh, M. Johir, J. Ren, H. K. Shon and L. D. Tijing, Recent Advances in High-Rate Solar-Driven Interfacial Evaporation, *Adv. Sci.*, 2024, **11**, 2401322.
92 J. Chen, D. Zhang, S. He, G. Xia, X. Wang, Q. Xiang, T. Wen, Z. Zhong and Y. Liao, Thermal insulation design for efficient and scalable solar water interfacial evaporation and purification, *J. Mater. Sci. Technol.*, 2021, **66**, 157–162.
93 Y. Tian and C.-Y. Zhao, A review of solar collectors and thermal energy storage in solar thermal applications, *Appl. Energy*, 2013, **104**, 538–553.
94 Z. Xu, Z. Li, Y. Jiang, G. Xu, M. Zhu, W.-C. Law, K.-T. Yong, Y. Wang, C. Yang and B. Dong, Recent advances in solar-driven evaporation systems, *J. Mater. Chem. A*, 2020, **8**, 25571–25600.
95 M. Chen, S. Li, D. Pang and H. Yan, Selective absorber and emitter boost water evaporation and condensation toward water collection, *Mater. Today Energy*, 2022, **28**, 101072.
96 F. Wang, C. Wang, G. Shi, Y. Wang, F. Li, K. Xu and M. Ma, Isolating solar harvesting and water evaporation of salt-free Janus steam generator for concentration-independent seawater desalination, *Desalination*, 2023, **545**, 116157.
97 J. Jiang, R. Yang, F. Zeng and S. Tu, Biomass-derived three-dimensional robust solar evaporator for efficient steam generation, water purification and salt-resistant desalination, *Chem. Eng. J.*, 2024, **481**, 148289.
98 Z. Yu, F. Li and Q. Xiang, Carbon dots-based nanocomposites for heterogeneous photocatalysis, *J. Mater. Sci. Technol.*, 2024, **175**, 244–257.
99 P. Du, Z. Chu, J. Zhang, J. Ma, F. Cao and J. Liu, Extraction of biomass carbon dots with peroxidase activity from peanut shells for visual sensing of edible cysteine, *Biomass Convers. Biorefin.*, 2024, **14**, 29009–29021.
100 V. Savchuk, R. Wang, L. Small and A. Pinchuk, Synergistic Effect in Hybrid Plasmonic Conjugates for Photothermal Applications, *ACS Omega*, 2024, **9**, 47436–47441.
101 X. Cui, Q. Ruan, X. Zhuo, X. Xia, J. Hu, R. Fu, Y. Li, J. Wang and H. Xu, Photothermal Nanomaterials: A Powerful Light-to-Heat Converter, *Chem. Rev.*, 2023, **123**, 6891–6952.
102 I. Primadona, F. A. Permatasari, M. A. Irham, M. Nasir and F. Iskandar, Recent advances and rational design strategies of carbon dots towards highly efficient solar evaporation, *Nanoscale*, 2021, **13**, 7523–7532.
103 Q. Hou, C. Xue, N. Li, H. Wang, Q. Chang, H. Liu, J. Yang and S. Hu, Self-assembly carbon dots for powerful solar water evaporation, *Carbon*, 2019, **149**, 556–563.
104 W. Chao, Y. Li, X. Sun, G. Cao, C. Wang and S.-H. Ho, Enhanced wood-derived photothermal evaporation system by in-situ incorporated lignin carbon quantum dots, *Chem. Eng. J.*, 2021, **405**, 126703.
105 J. Yang, D. Liu, X. Song, Y. Zhao, Y. Wang, L. Rao, L. Fu, Z. Wang, X. Yang, Y. Li and Y. Liu, Recent Progress of Cellulose-Based Hydrogel Photocatalysts and Their Applications, *Gels*, 2022, **8**, 270.
106 M. N. A. S. Ivan, S. Saha, A. M. Saleque, S. Ahmed, A. K. Thakur, G. Bai, Z. Miao, R. Saidur and Y. H. Tsang, Progress in interfacial solar steam generation using low-dimensional and biomass-derived materials, *Nano Energy*, 2024, **120**, 109176.
107 X. Guo, S. Cheng, W. Cai, Y. Zhang and X.-A. Zhang, A review of carbon-based thermal interface materials: Mechanism, thermal measurements and thermal properties, *Mater. Des.*, 2021, **209**, 109936.
108 I. Rahmawati, Indriyati, F. A. Permatasari, M. A. Irham, M. I. Nugraha, T. D. Anthopoulos and F. Iskandar, Modulating Photothermal Properties of Carbon Dots through Nitrogen Incorporation Enables Efficient Solar Water Evaporation, *ACS Appl. Nano Mater.*, 2023, **6**, 2517–2526.

109 Z. Wang, W. Tu, Y. Zhao, H. Wang, H. Huang, Y. Liu, M. Shao, B. Yao and Z. Kang, Robust carbon-dot-based evaporator with an enlarged evaporation area for efficient solar steam generation, *J. Mater. Chem. A*, 2020, **8**, 14566–14573.
110 Y. Tian, X. Liu, S. Xu, J. Li, A. Caratenuto, Y. Mu, Z. Wang, F. Chen, R. Yang, J. Liu, M. L. Minus and Y. Zheng, Recyclable and efficient ocean biomass-derived hydrogel photothermal evaporator for thermally-localized solar desalination, *Desalination*, 2022, **523**, 115449.
111 H. Zhang, X. Li, X. Liu, Y. Du, W. Xie, S. Zheng, L. Yang, J. Shi and D. Jing, Biomimetic hydrogel with directional heat regulation for efficient solar desalination, *Chem. Eng. J.*, 2023, **473**, 145484.
112 Y.-L. He, C.-H. Zhou, Z. Chen, I. Rimeh, L. Xing, A. Yimingniyazi, A. Parkash, P.-C. Ma and A. Kadier, Invasive plant-derived carbon dots and carbon black co-deposited basalt fiber fabric as an efficient solar interface evaporator for high salinity water purification, *Sep. Purif. Technol.*, 2025, **365**, 132644.
113 A. R. Pati, Y. S. Ko, C. Bae, I. Choi, Y. J. Heo and C. Lee, Highly porous hydrogels for efficient solar water evaporation, *Soft Matter*, 2024, **20**, 4988–4997.
114 E. M. Ahmed, Hydrogel: Preparation, characterization, and applications: A review, *J. Adv. Res.*, 2015, **6**, 105–121.
115 H. Zhang, D. Xu, Y. Zhang, M. Li and R. Chai, Silk fibroin hydrogels for biomedical applications, *Smart Med.*, 2022, **1**, e20220011.
116 T. Dutta, P. Chaturvedi, I. Llamas-Garro, J. S. Velázquez-González, R. Dubey and S. K. Mishra, Smart materials for flexible electronics and devices: hydrogel, *RSC Adv.*, 2024, **14**, 12984–13004.
117 W. Gao, M. Zhong and B. Su, Hydrogel-Based Photocatalysts: Applications in Environmental Remediation and Energy Conversion, *J. Polym. Environ.*, 2024, **32**, 6131–6148.
118 L. Zhu, L. Tian, S. Jiang, L. Han, Y. Liang, Q. Li and S. Chen, Advances in photothermal regulation strategies: from efficient solar heating to daytime passive cooling, *Chem. Soc. Rev.*, 2023, **52**, 7389–7460.
119 Y. Shi, A. Feng, S. Mao, C. Onggowarsito, X. S. Zhang, W. Guo and Q. Fu, Hydrogels in solar-driven water and energy production: Recent advances and future perspectives, *Chem. Eng. J.*, 2024, **492**, 152303.
120 X. Xu, N. Guillomaitre, K. S. S. Christie, R. K. Bay, N. Bizmark, S. S. Datta, Z. J. Ren and R. D. Priestley, Quick-Release Antifouling Hydrogels for Solar-Driven Water Purification, *ACS Cent. Sci.*, 2023, **9**, 177–185.
121 M. E. Mashhadi, M. M. Hassan, R. Yang and Q. Lu, All-in-One Hybrid Solar-Driven Interfacial Evaporators for Cogeneration of Clean Water and Electricity, *Adv. Funct. Mater.*, 2024, **35**, 2412870.
122 C. Li, B. Zhu, Z. Liu, J. Zhao, R. Meng, L. Zhang and Z. Chen, Polyelectrolyte-based photothermal hydrogel with low evaporation enthalpy for solar-driven salt-tolerant desalination, *Chem. Eng. J.*, 2022, **431**, 134224.
123 A. Ni, D. Fu, P. Lin, X. Wang, Y. Xia, X. Han and T. Zhang, Eco-friendly photothermal hydrogel evaporator for efficient solar-driven water purification, *J. Colloid Interface Sci.*, 2023, **647**, 344–353.
124 Y. Liu and X. Zheng, 3D printed thermo-responsive hydrogel evaporator with enhanced water transport for efficient solar steam generation, *Sol. Energy*, 2024, **273**, 112507.
125 R. Li, Y. Liu, J. He, C. Zhang, J. Bai, Y. Sun, W. Diao and X. Tang, Superhydrophilic hydrogel with adjustable vertical channels and low water evaporation enthalpy for efficient solar evaporation, *Desalination*, 2025, **610**, 118841.
126 B. Huang, J. Liu, J. Xie, R. Tang, H. Zhu, B. Peng and W. Zhang, Enhancement of solar water evaporation in copper-sodium humate/SA/PAM hydrogels via an environmental heat field, *Sep. Purif. Technol.*, 2025, **366**, 132784.
127 J. Jiang, H. Jin, Y. Lu, X. Liu, H. Ge and L. Mu, Hydrogel-engineered platforms for efficient solar interfacial evaporation: Current status and future directions, *J. Water Process Eng.*, 2025, **78**, 108735.
128 Y. Liu, S. Shen, Z. Duan, J. Deng and D. Fan, Hydrogels for Long-Term Moisture Retention under Ambient Conditions: Inhibiting the Evaporation of Free Water from Macroscopic to Molecular Scales, *Adv. Funct. Mater.*, 2025, **35**, 2504356.
129 H. Yang, W. Lei, H. Yang, Y. Xiong, C. Liu, Y. Han, Z. Z. Yu and X. Li, One-Step In Situ Synthesis of a Reduced Graphene Oxide-Based Hybrid Hydrogel for Highly Efficient Water Evaporation and Comprehensive Wastewater Treatment, *ACS Appl. Mater. Interfaces*, 2025, **17**, 46046–46058.
130 N. An, M. Ma, Y. Chen, Z. Wang and Q. Li, Biomass Hydrogel Solar-Driven Multifunctional Evaporator for Desalination, VOC Removal, and Sterilization, *ACS ES&T Eng.*, 2025, **5**, 732–742.
131 R. Foudazi, R. Zowada, I. M. Zloczower and D. L. Feke, Porous Hydrogels: Present Challenges and Future Opportunities, *Langmuir*, 2023, **39**, 2092–2111.
132 Z. Feng, C. Feng, N. Chen, W. Lu and S. Wang, Preparation of composite hydrogel with high mechanical strength and reusability for removal of Cu(II) and Pb(II) from water, *Sep. Purif. Technol.*, 2022, **300**, 121894.
133 Y. H. Wang, C. C. Hsu, S. H. Hong, J. F. Ding, U. S. Jeng, D. Y. Kang, S. C. Luo, S. H. Tung and C. L. Liu, A Dual-Function Poly (vinyl alcohol) Hydrogel for Solar Water Production and Thermoelectric Energy Generation, *ACS Sustainable Chem. Eng.*, 2025, **13**, 4231–4241.
134 B. Meera, C. Vidhya, R. B. Nair, R. Surya and S. Kurian, Sustainable sponge-like composite hydrogel evaporator for highly efficient solar steam generation, *Mater. Today Sustainability*, 2023, **23**, 100439.
135 Q. Yin, J. Zhang, Y. Tao, F. Kong and P. Li, The emerging development of solar evaporators in materials and structures, *Chemosphere*, 2022, **289**, 133210.
136 S. Jiang, Z. Zhang, T. Zhou, S. Duan, Z. Yang, Y. Ju, C. Jia, X. Lu and F. Chen, Lignin hydrogel-based solar-driven evaporator for cost-effective and highly efficient water purification, *Desalination*, 2022, **531**, 115706.
137 S. Mao, M. A. H. Johir, C. Onggowarsitto, A. Feng, L. D. Nghiem and Q. Fu, Functionalized Boron Nitride

Nanomaterials: Exploring Antioxidant Activity and Cellular Responses, *Mater. Adv.*, 2022, **3**, 1322–1340.

138 X. Zhang, L. Sun, X. Wang, S. Zou, C. Cao, J. Hou, F. Guo, C. Li and W. Shi, Hydrogel-based 3D evaporator with cross-linked fixation by carbon dots for ultra-high and stable solar steam generation, *J. Chem. Eng.*, 2024, **497**, 154793.

139 M. Wang, G. Xu, Y. Wu, R. R. Gonzales, K. Xu, H. Zhao and F. Wang, Engineering hydrogels towards next-generation multifunctional interfacial solar evaporators beyond seawater desalination, *J. Chem. Eng.*, 2024, **502**, 157988.

140 B. Huang, R. Tang, X. Zheng, G. Chen, Q. Li, W. Zhang and B. Peng, Structurally regulated hydrogel evaporator with excellent salt-resistance for efficient solar interfacial water evaporation, *J. Environ. Chem. Eng.*, 2024, **12**, 111827.

141 A. K. Kaviti, J. S. G. Balaji, A. S. Ram and A. A. Kumari, An overview on hydrogel materials for solar desalination, *Mater. Today: Proc.*, 2021, **44**, 2526–2532.

142 Z. Li, A. Nabhai, O. C. Wasson, I. S. Mainardi, J. Wang, J. Springstead, Q. Wu and J. Li, Transformation from Hydrogels to Nanostructured Aerogels: Review and Future Perspectives, *ACS Appl. Nano Mater.*, 2025, **8**, 13954–13974.

143 K. Sharma, P. Choudhary, A. Majeed, S. Guleria, M. Kumar, A. K. Rana and G. Rajauria, Cellulose based membranes, hydrogels and aerogels for water treatment application, *Ind. Crops Prod.*, 2025, **225**, 120474.

144 S. W. Sharshir, A. M. Algazzar, K. A. Elmaadawy, A. W. Kandeal, M. R. Elkadeem, T. Arunkumar, J. Zang and N. Yang, New hydrogel materials for improving solar water evaporation, desalination and wastewater treatment: A review, *Desalination*, 2020, **491**, 114564.

145 H. Yin, F. Liu, T. Abdiryim and X. Liu, Self-Healing Hydrogels: From Synthesis to Multiple Applications, *ACS Mater. Lett.*, 2023, **5**, 1787–1830.

146 S. Nayak, S. R. Prasad, D. Mandal and P. Das, Carbon dot cross-linked polyvinylpyrrolidone hybrid hydrogel for simultaneous dye adsorption, photodegradation and bacterial elimination from waste water, *J. Hazard. Mater.*, 2020, **392**, 122287.

147 X. Wei, X. Wang, Y. Fu, X. Zhang and F. Yan, Emerging trends in CDs@hydrogels composites: from materials to applications, *Microchim. Acta*, 2024, **191**, 355.

148 F. Cui, L. Xi, D. Wang, L. Ren, X. Tan, X. Li, J. Li and T. Li, Advanced in carbon dot-based hydrogels for antibacterial, detection and adsorption, *Coord. Chem. Rev.*, 2023, **497**, 215457.

149 P. K. Marvi, P. Das, A. Jafari, S. Hassan, H. Savoji, S. Srinivasan and A. R. Rajabzadeh, Multifunctional Carbon Dots In Situ Confined Hydrogel for Optical Communication, Drug Delivery, pH Sensing, Nanozymatic Activity, and UV Shielding Applications, *Adv. Healthcare Mater.*, 2025, **14**, 2403876.

150 S. Singh, N. Shauloff and R. Jelinek, Solar-Enabled Water Remediation *via* Recyclable Carbon Dot/Hydrogel Composites, *ACS Sustainable Chem. Eng.*, 2019, **7**, 13186–13194.

151 M. Li, M. Yang, B. Liu, H. Guo, H. Wang, X. Li, L. Wang and T. D. James, Self-assembling fluorescent hydrogel for highly efficient water purification and photothermal conversion, *J. Chem. Eng.*, 2022, **431**, 134245.

152 Indriyati, D. F. S. Ramadhani, F. A. Permatasari, M. M. Munir, M. Nasir and F. Iskandar, Flexible Photothermal Membrane Based on PVA/Carbon Dot Hydrogel Films for High-Performance Interfacial Solar Evaporation, *ACS Appl. Polym. Mater.*, 2024, **6**, 6726–6736.

153 X. Jing, L. Chen, Y. Li, H. Yin, J. Chen, M. Su, F. Liu, T. Abdiryam, F. Xu, J. You and X. Liu, Synergistic Effect Between 0D CQDs and 2D MXene to Enhance the Photothermal Conversion of Hydrogel Evaporators for Efficient Solar Water Evaporation, Photothermal Sensing and Electricity Generation, *Small*, 2024, **20**, 2405587.

154 G. Liu, Q. Ma, Z. Li, J. Zheng Li, J. Zhang, K. Lei, D. Li, M. Xue, W. Wu, J. Du and X. Zhang, Dual-functional hydrogel evaporator with CQDs loaded TiO_2 and CNTs for efficient eutrophic water body purification, *Desalination*, 2026, **622**, 119752.

155 Y. Sun, D. Qu, W. Liu, L. An, X. Wang and Z. Sun, Fabrication of a bilayer structural carbon-based hydrogel material with excellent energy conversion efficiency, *Sci. China Mater.*, 2023, **66**, 4834–4840.

156 N. An, M. Ma, Y. Chen, Z. Wang and Q. Li, Biomass Hydrogel Solar-Driven Multifunctional Evaporator for Desalination, VOC Removal, and Sterilization, *ACS ES&T Eng.*, 2025, **5**, 732–742.

157 N. An, R. Su, Z. Wang, W. Chen, W. Zhou and Q. Li, Hydrogel-based photothermal evaporator for efficient solar desalination and synergistic removal of volatile organic compounds, *Desalination*, 2023, **565**, 116849.

158 J. Li, C. Li, L. Chen, T. Li, F. Gao, X. Chen, T. Zhao, F. Wang and Y. Jiang, A gradient photothermal hydrogel with carbon-dots deposited molybdenum disulfide nanoflowers as photothermal centres for efficient solar-driven water evaporation and treatment, *Surf. Interfaces*, 2024, **55**, 105433.

159 L. Li, C. Xue, Q. Chang, X. Ren, N. Li, J. Yang, S. Hu and H. Xu, Polyelectrolyte Hydrogel-Functionalized Photothermal Sponge Enables Simultaneously Continuous Solar Desalination and Electricity Generation Without Salt Accumulation, *Adv. Mater.*, 2024, **36**, 2401171.

160 X. Xu, Q. Chang, C. Xue, N. Li, H. Wang, J. Yang and S. Hu, A carbonized carbon dot-modified starch aerogel for efficient solar-powered water evaporation, *J. Mater. Chem. A*, 2022, **10**, 11712–11720.

161 M. Fargharazi and M. M. Bagheri-Mohagheghi, PVA:GA polymer hydrogel/activated carbon (AC) nanocomposite as solar photothermal materials: study of structural, optical absorption and water purification properties, *J. Mater. Sci.: Mater. Electron.*, 2024, **35**, 449.

162 G. Liu, H. Chang, H. Deng, Y. Wang, D. Wang, Q. Zhang, Q. Jiang and Z. Liu, Enhancing the photothermal performance of polydopamine with sludge-based carbon dots and constructing a solar evaporation system with catalytic performance, *Renewable Energy*, 2026, **258**, 125055.

163 H. Huo, J. Shen, J. Wan, H. Shi, H. Yang, X. Duan, Y. Gao, Y. Chen, F. Kuang, H. Li, L. Yang and G. Du, A tough and

robust hydrogel constructed through carbon dots induced crystallization domains integrated orientation regulation, *Nat. Commun.*, 2025, **16**, 6221.

164 S. W. Park, S. H. Im, W. T. Hong, H. K. Yang and Y. K. Jung, Lignin-derived carbon quantum dot/PVA films for totally blocking UV and high-energy blue light, *Int. J. Biol. Macromol.*, 2024, **268**, 131919.

165 M. Chen, M. Zhou, Y. Wang, C. Mao, S. Pang, T. Meng and X. Yang, Carboxymethyl cellulose and sodium alginate-enhanced hydrogel for carbon dots loading: A novel platform for pH sensing and sensitive detection of Al^{3+} and Ag+, *Int. J. Biol. Macromol.*, 2025, **307**, 141955.

166 T. Zhang, J. Yang, Y. Yang, C. Li, X. Xu, Z. Z. Yu and X. Li, Deformation-resistant sponge-like hydrogel evaporators for efficient solar steam generation and high salinity desalination, *Desalination*, 2025, **602**, 118599.

167 X. Zhang, L. Sun, X. Wang, S. Zou, C. Cao, J. Hou, F. Guo, C. Li and W. Shi, Hydrogel-based 3D evaporator with cross-linked fixation by carbon dots for ultra-high and stable solar steam generation, *J. Chem. Eng.*, 2024, **497**, 154793.

168 N. Mate, K. Prakash, K. Nabeela and S. M. Mobin, Organic Network Comprising Sustainable Carbon Dots Upgraded Bacterial Cellulose Evaporator for Interfacial Solar-Driven Water Evaporation, *ACS Mater. Lett.*, 2025, **7**, 2413–2421.